(9)

PRODUCTION OF A PLASMA WITH HIGH-LEVEL PULSED MICROWAVE POWER

THOMAS J. FESSENDEN

TECHNICAL REPORT 389

AUGUST 29, 1961

MASSACHUSETTS INSTITUTE OF TECHNOLOGY
RESEARCH LABORATORY OF ELECTRONICS
CAMBRIDGE, MASSACHUSETTS

MASSACHUSETTS INSTITUTE OF TECHNOLOGY
RESEARCH LABORATORY OF ELECTRONICS

Technical Report 389 August 29, 1961

PRODUCTION OF A PLASMA WITH HIGH-LEVEL PULSED MICROWAVE POWER

Thomas J. Fessenden

This report is based on a thesis submitted to the Department of Electrical Engineering, M.I.T., April 29, 1961, in partial fulfillment of the requirements for the degree of Master of Science.

Abstract

A method is presented for producing a dense plasma in a resonant cavity with microwave energy. The plasma is contained in a quartz tube lying along the axis of a resonant cavity that is excited near the TE_{111} coaxial-mode resonance with 10-μsec pulses of up to 800 kw of peak power in the 10-cm band. The plasma serves as a center conductor for the coaxial mode, shifting the mode resonance near the exciting frequency. The initial transient in the plasma electron density occurs very rapidly, and the system appears to reach a steady state in less than 10 μsec. A second microwave system excites the cavity in the TE_{011} coaxial mode, which is used as a low-level probe to measure the properties of the plasma.

A perturbation formula is developed that can be used to calculate the perturbing effects of the dense plasma. This formula is used to develop methods of calculating the electron density and collision frequency of the plasma by measurements of the detuning of the cavity mode. Plasma electron densities of over $10^{14}/cm^3$ are measured when over 80 kw of peak power are dissipated in the discharge. Studies are also presented of helium discharges and of light generated by the discharges.

TABLE OF CONTENTS

I. INTRODUCTION AND INITIAL CONSIDERATIONS

1.1 PURPOSE

This work considers a method of producing and measuring a dense plasma in a resonant cavity. Produced by pulsed microwave power, the plasma is studied only when the microwave power is present. It was hoped that the parameters of the system would reach a steady state in the time of the microwave pulse so that a steady-state plasma produced by very large microwave power levels could be studied. There is a considerable amount of experimental evidence that a steady-state condition was nearly reached and that the only transients that were occurring at the time of the measurements were the relatively slow thermal transients. However, further experiments using longer microwave pulses are necessary to determine if this were the case.

1.2 HISTORY OF THE PROBLEM

One of the most useful methods of measuring the properties of a plasma is to introduce the plasma into a resonant cavity and measure the detuning of the cavity which the plasma produces. This technique was developed by Rose, Kerr, Biondi, Everhart, and Brown[1] in 1949 and is discussed by Rose and Brown.[10] The method uses a perturbation formula derived by Slater[2] in 1946 to relate the cavity detuning to the electron density and collision frequency of the plasma. The resonant-cavity method is valid for low plasma electron densities. The electron density that produces plasma resonance at the excitation frequency is the approximate upper limit of this technique. Limits of the microwave-cavity method are discussed by Persson.[3] Buchsbaum and Brown[4] have shown that, if the electric field of the cavity mode is perpendicular to the electron-density gradients in the plasma, the resonant-cavity method can be extended by a factor of approximately 10 to higher densities.

The condition of plasma resonance limits a 10-cm band system to the measurement of plasmas that have an electron density not greater than approximately $10^{12}/cm^3$ if the simple perturbation theory is used. For the measurement of larger plasma electron densities, it has been necessary to calculate exactly the cavity resonant frequency as a function of the electron density of the plasma. These calculations have been performed for the TM_{010}, TM_{020}, and TE_{011} cylindrical-cavity modes as a function of the density of a lossless, uniform plasma column along the cavity axis by Buchsbaum, Mower, and Brown.[4,5]

Hsieh, Goldey, and Brown[6] calculated the detuning of a resonant cavity, including loss. They were interested in the effects a small semiconducting rod along the axis of a cylindrical, resonant cavity produced on the resonant frequency and Q of the TM_{010} mode. They found that, as the electron density in the semiconductor increases, the cavity Q first decreases to a very low value and then increases to

approximately its original value at infinite electron density. The cavity resonant frequency increases continuously, but not linearly, after the minimum Q point is reached. Physically, at low electron densities, the semiconductor does not greatly perturb the cavity fields and the fields are very nearly those of the TM_{010} cylindrical waveguide cavity mode. As the electron density increases, the semiconductor begins to exclude the microwave fields from its interior until, at infinite electron density, the microwave field does not penetrate the semiconductor, and the cavity fields are those of the TM_{010} coaxial mode.

A plasma rod in which collisions are important, and which lies along the axis of a cylindrical cavity, will perturb the parameters of the TM_{010} mode in precisely the same way as the semiconducting rod. Thus, the plasma changes from a medium that resembles a lossy dielectric at low electron densities to one that resembles a lossy conductor at high densities. This same conclusion can be reached by considering the simpler problem of plane wave reflection from a semi-infinite plasma. This problem has been considered by Buchsbaum.[7]

Several experimental techniques of measuring the change in Q value and resonant frequency of a resonant cavity have been developed by Rose and Brown[8-10] and Gould and Brown.[11]

The ease of analyzing the perturbing effects of a tenuous plasma on the parameters of a resonant cavity has led to the development of an experimental technique for measuring several of the basic parameters of a plasma. The plasma is produced by a short microwave pulse and allowed to decay until thermal equilibrium is reached. Measurements of the rate of decay of the electron density are then used to calculate the diffusion, attachment, or recombination coefficient of the gas, depending on which process is predominant. The experimental technique is described by Biondi and Brown.[12] The collision frequency of the decaying plasma may also be measured accurately during the afterglow period. This technique was used by Phelps, Fundingsland, and Brown[13] to measure the electron collision frequency of hydrogen. The experimental advantage of performing experiments in the afterglow is that both the electron temperature and density distribution are known once thermal equilibrium has been reached. Therefore, none of the experimenters using this technique studied the plasma when the driving pulse was present.

An interesting experiment was studied by Everhart, Allis, and Brown.[14,15] A discharge was produced in a parallel-plate geometry by high-frequency energy. The complex admittance of the discharge was measured as a function of the parameters of the high-frequency energy. They found that the electron density in the plasma was proportional to the conduction current in the plasma until the plasma conduction current was approximately equal to the displacement current between the plates. At this point, the relation became nonlinear. Observations of the light generated by the discharge showed that, under nonlinear operation, the light was brightest in a region near each plate. As the discharge power was increased, the bright region moved nearer each

parallel plate. A theoretical analysis showed that their original assumption of a uniform electric field between the plates was no longer valid and that the electric-field intensity and the ionization frequency were greatest in the bright regions. The electron density in the bright regions was that required to produce plasma resonance at the excitation frequency. At low densities, the plasma was in its lowest diffusion mode and the electron density varied sinusoidally between the plates. As the electron density increased, the variation remained sinusoidal until the plasma-resonance condition was reached. As more power was placed in the discharge, the bright regions appeared and the plasma density became more uniform.

A hydrogen discharge in a resonant cavity which was produced by the fields of the TM_{010} mode was studied by Rose and Brown.[16] The plasma was contained in a quartz bottle that partially filled the cavity. By considering the transition from free to ambipolar diffusion with increasing density, they were able to calculate the electric field required to maintain the discharge as a function of the electron density and neutral-gas pressure. They performed experiments which agreed satisfactorily with their theory. The electron density of the plasma studied by Rose and Brown was always much lower than that which produces plasma resonance at the excitation frequency.

Buchsbaum[17] attempted to produce a dense plasma in a resonant cavity using a 1000-watt cw microwave source. The geometry of his resonant cavity and the method of containing the discharge was almost identical to that described in this report. The principal difference is that Buchsbaum used an axial magnetic field to couple the discharge more efficiently to the source, and no magnetic field was used in the experiments of this report. Buchsbaum had difficulty in coupling a large portion of the incident microwave energy into the discharge because the plasma loaded the cavity mode and decoupled the cavity from the source. He obtained a density of $6 \times 10^{11}/cm^3$ with 30 watts of microwave power dissipated in the discharge.

A pulsed microwave discharge produced in a resonant cavity was studied by Madan, Gordon, Buchsbaum, and Brown.[18] They used measurements of the rate at which the plasma electron density increased to calculate the diffusion coefficient and ionization frequency of a hydrogen discharge. They showed that the electron density of the discharge increases very rapidly when the microwave pulse is applied – particularly at large pulsed-power levels.

The experimental results and theories of these workers were used to develop the theoretical and experimental techniques described in this report.

A simple theory is used to calculate the detuning of a cavity mode which is caused by a gas discharge produced by the cavity fields. The electron density of the plasma is assumed to be uniform over the volume occupied by the plasma. This assumption is an approximation to the real situation, for it can be shown that this assumption leads to an infinite-loss rate of electrons from the plasma by the process of diffusion. However, the work of Everhart, Allis, and Brown[14, 15] indicates that, for the purposes of calculating the microwave interaction with the plasma, assuming the plasma to be uniform is

better than assuming, as is sometimes done, the plasma to be in the lowest-order diffusion mode.

In the theoretical work that follows, complex notation is used. All ac quantities are assumed to vary as $e^{j\omega t}$. The actual time-dependence of the ac quantities can be found by multiplying their complex values by $e^{j\omega t}$ and taking the real part of the result.

II. MEASUREMENT OF A DENSE PLASMA IN A RESONANT CAVITY

2.1 INTRODUCTION

In this section, the theory is developed for measuring the electron density and collision frequency of a dense plasma in a resonant cavity. The theory uses a perturbation technique that is based on Slater's perturbation formula for cavities.[2] The theory differs from that used by previous workers[1, 8-11] in that the electron density of the plasma is assumed to be infinite rather than zero in the unperturbed state. In this assumption the plasma appears as a perfect conductor and forms part of the wall of the resonant cavity. The effects of a finite, but large, plasma electron density are then treated with the perturbation formula in the same way as the effects of loss in a metal cavity wall are treated.

In the following considerations, it is assumed that the electron density and collision frequency of the plasma are constant over the volume occupied by the plasma. These are rather severe assumptions, for, in general, density gradients will exist both parallel and perpendicular to the plasma boundary. To partially avoid this difficulty, a geometrically weighted electron density is defined which reduces to the correct value in the limit of uniform density. The weighted density considers only the variations of electron density which are parallel to the plasma surface. The assumption of constant collision frequency requires that the collision frequency be independent of the electron energy. Such is the case for electron-neutral collisions in helium[19] and hydrogen[13] at electron energies above approximately 4 volts.

The results of the analysis of a dense plasma in a resonant cavity are used to develop a method of calculating the plasma parameters by measuring the detuning of a cavity mode which is caused by the plasma. Two experimental techniques are considered. In the first technique, the plasma is produced by some external means and then probed with a low-power cavity mode. In the second experimental method, the plasma is produced by the microwave fields in the cavity.

2.2 THE PLASMA WALL

Because it is a collection of neutral and charged particles, an ionized gas or plasma will react under the influence of an electromagnetic field. Therefore, a plasma medium is describable by a permeability μ, a permittivity ϵ, and a conductivity σ. The expressions for these quantities are

$$\mu = \mu_o \tag{1}$$

$$\epsilon = \epsilon_o \tag{2}$$

and

$$\sigma = \frac{ne^2}{m} \frac{1}{\nu_c + j\omega} \tag{3}$$

where μ_o and ϵ_o are the permeability and permittivity of free space, n is the electron density, e is the electronic charge, ω is the applied angular frequency, ν_c is the collision frequency for momentum transfer, and m is the mass of an electron.

These equations are subject to the assumptions that (a) The collision frequency is independent of electron energy; (b) The ions are not directly affected by the electromagnetic field, and (c) The effects of the interaction of the electrons with the ac magnetic field are negligible.

The first assumption is justified if helium or hydrogen is used as the gas. The second assumption will always hold true because the power absorbed by a species of particle is inversely proportional to the mass of the particle; that is, the electron, having much less mass, will be affected much more strongly by the microwave field than the ion. The third assumption will generally hold true.

It is convenient to define two parameters, a normalized density variable η and a normalized collision-frequency variable γ, by the equations

$$\eta \equiv \left(\frac{\omega_p}{\omega}\right)^2 = \frac{ne^2}{m\epsilon_o\omega^2} \tag{4}$$

and

$$\gamma \equiv \frac{\nu_c}{\omega} \tag{5}$$

where ω_p is a parameter that frequently appears in plasma work and is called the plasma frequency.

Combining Eqs. 4 and 5, we obtain

$$\sigma = \frac{\omega\epsilon_o\eta(\gamma - j)}{1 + \gamma^2} \tag{6}$$

This is a more convenient form and is the one that will be used.

Let us consider a plane wave that is propagating in the plasma medium. From Maxwell's equations, we readily find that the intrinsic impedance of the plasma is given by

$$Z_p = \frac{|\overline{E}|}{|\overline{H}|} = \left[\frac{j\omega\mu_o}{\sigma + j\omega\epsilon_o}\right]^{1/2} \tag{7}$$

where $\overline{E}$ is the electric-field intensity and $\overline{H}$ is the magnetic-field intensity in the plasma. Similarly, the propagation constant Γ of a uniform plane wave in a plasma is found to be

$$\Gamma = [j\omega\mu_o(\sigma+j\omega\epsilon_o)]^{1/2} \tag{8}$$

By substituting Eq. 6 in Eqs. 7 and 8, we obtain

$$Z_p = \left(\frac{\mu_o}{\epsilon_o}\right)^{1/2} \left(\frac{1-j\gamma}{1-\eta-j\gamma}\right)^{1/2} \tag{9}$$

and

$$\Gamma = j\frac{\omega}{c}\left(1-\frac{\eta}{1-j\gamma}\right)^{1/2} \tag{10}$$

where c is the velocity of light.

Note that if the collision frequency is zero and η is greater than one, the intrinsic impedance of the plasma is pure imaginary and the propagation constant is pure real. Under these conditions, the medium is cut off, and the fields in the plasma decay exponentially with distance. Following Buchsbaum,[7] we define an equivalent skin depth δ in the plasma as the distance in which a plane wave decays by a factor of 1/e. In terms of the propagation constant, δ is given by

$$\delta = -\frac{1}{\text{Re } \Gamma} \tag{11}$$

Considering Eqs. 9-11 in the limit of large η, we obtain

$$Z_p = j\left(\frac{\mu_o}{\epsilon_o}\right)^{1/2} \left(\frac{1-j\gamma}{\eta}\right)^{1/2} \tag{12}$$

$$\Gamma = -\frac{\omega}{c}\left(\frac{\eta}{1-j\gamma}\right)^{1/2} \tag{13}$$

$$\delta = \frac{c}{\omega}\left(\frac{\eta}{1+\gamma^2}\right)^{1/2} \frac{1}{\text{Re } (1+j\gamma)^{1/2}} \tag{14}$$

2.3 REFLECTION FROM A PLASMA WALL

Consider a uniform plane wave normally incident on a semi-infinite plasma of uniform density n as illustrated in Fig. 1.

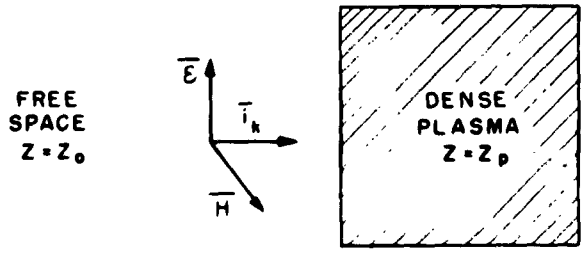

Fig. 1. Orientation of a uniform plane wave normally incident on a semi-infinite plasma.

Let the incident wave be denoted by subscript i, the reflected wave by subscript r, and the transmitted wave by subscript t. The requirements of Maxwell's equations that both the tangential electric field $\overline{E}$ and magnetic field $\overline{H}$ be continuous at the plasma boundary lead to the equations

$$\overline{E}_i + \overline{E}_r = \overline{E}_t \tag{15}$$

and

$$\overline{H}_i + \overline{H}_r = \overline{H}_t \tag{16}$$

The fields $\overline{E}_i$ and $\overline{H}_i$ are related by the equation

$$\overline{H}_i = (1/Z_o)\, \bar{i}_k \times \overline{E}_i \tag{17}$$

Similarly,

$$\overline{H}_r = -\frac{1}{Z_o}\, \bar{i}_k \times \overline{E}_r \tag{18}$$

and

$$\overline{H}_t = \frac{1}{Z_p}\, \bar{i}_k \times \overline{E}_t \tag{19}$$

where Z_p is the intrinsic impedance of the plasma and is given in Eq. 8, and where Z_o is the intrinsic impedance in medium I, which for free space is

$$Z_o = \left(\frac{\mu_o}{\epsilon_o}\right)^{1/2} \tag{20}$$

From Eqs. 15-20, we obtain

$$\overline{E}_t = \frac{2\overline{E}_i}{1 + [1-\eta/(1-j\gamma)]^{1/2}} \tag{21}$$

$$\overline{E}_r = \left[\frac{2}{1 + [1-\eta/(1-j\gamma)]^{1/2}} - 1\right] \overline{E}_i \tag{22}$$

and

$$\overline{H}_t = \frac{2\overline{H}_i}{1 + 1/[1-\eta/(1-j\gamma)]^{1/2}} \tag{23}$$

$$\overline{H}_r = \left[\frac{2}{1 + 1/[1-\eta/(1-j\gamma)]^{1/2}} - 1\right] \overline{H}_i \tag{24}$$

These equations indicate that, in the limit of infinite electron density ($\eta = \infty$), the plasma wall appears to be a perfect conductor and an incident plane wave is perfectly reflected.

If the electron density is large, but not infinite, Eqs. 21-24 are given approximately by

$$\overline{E}_t \simeq \frac{j(1-j\gamma)^{1/2}}{\eta^{1/2}} 2\overline{E}_i \tag{25}$$

$$\overline{E}_r \simeq -\overline{E}_i \tag{26}$$

$$\overline{H}_t \simeq 2\overline{H}_i \tag{27}$$

$$\overline{H}_r \simeq \overline{H}_i \tag{28}$$

Equations 25-28 state that in the limit of large η, the $\overline{H}$ field that exists at the plasma wall is approximately equal to the fields which would exist if the plasma were replaced by a perfect conductor. We shall use this fact in the next section when we consider the effects of a plasma wall on a resonant cavity.

These equations have been derived by considering plane wave reflection from a semi-infinite plasma. They may be directly applied to a plasma of finite dimensions if the plasma skin depth δ given in Eq. 14 is much less than any plasma dimension.

The above analysis assumes that the plasma electron density rises from zero to its maximum value at the plasma surface; this rise requires an infinite electron-density gradient at the plasma surface. Using diffusion theory,[20] we can prove that the electron-density gradient must be finite at the plasma surface, and, thus, the above analysis may be questioned. However, since the analysis in section 2.4 is not exact, we shall assume that the simple analysis presented here is valid.

2.4 PERTURBATION OF A RESONANT CAVITY BY A PLASMA WALL

Consider a resonant cavity composed of a volume of space that is surrounded in part S' by a good conductor and in part S" by a dense plasma, as in Fig. 2. Here a dense plasma is one in which the normalized density parameter η is much greater than unity.

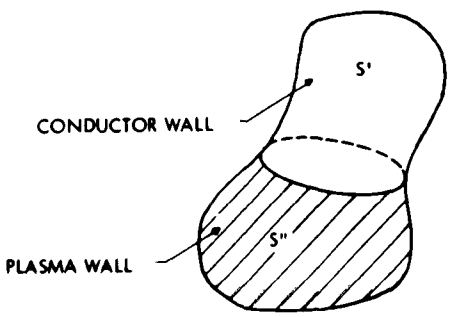

Fig. 2. General cavity enclosed by a conducting wall S' and a plasma wall S".

In the previous section, we saw that a dense plasma has many properties of a good conductor; therefore, the effects of the plasma wall on the properties of a resonant cavity can be calculated in the same way as the effects of good, but not perfect, wall conductors are obtained. The following work closely parallels that done by Slater[21] who used a perturbation technique to calculate the detuning of a resonant cavity which was caused by

imperfectly conducting metal cavity wall.

Let $\bar{E}$ and $\bar{H}$ represent the electric and magnetic fields which exist in the cavity of Fig. 2. At the resonant frequency of the cavity, we have

$$\nabla \times \bar{E} = -s\mu_o \bar{H} \tag{29}$$

$$\nabla \times \bar{H} = s\epsilon_o \bar{E} \tag{30}$$

Here, s is the complex resonant frequency of the cavity and is given by

$$s = -1/\tau + j\omega' \tag{31}$$

where τ is the characteristic decay time and ω' is the angular frequency of the cavity fields.

Next, let $\bar{E}_o$ and $\bar{H}_o$ represent the electric and magnetic fields that exist in the cavity of Fig. 2 with both walls, S" and S', replaced by perfect conductors. At the resonant frequency ω'_o of the lossless cavity, Maxwell's equations are

$$\nabla \times \bar{E}_o = -j\omega'_o \mu_o \bar{H}_o \tag{32}$$

and

$$\nabla \times \bar{H}_o = j\omega'_o \epsilon_o \bar{E}_o \tag{33}$$

After some manipulation, we obtain, from Eqs. 29, 30, 32 and 33,

$$s - j\omega'_o = - \frac{\oint_S \bar{E} \times \bar{H}_o^* \cdot d\bar{a}}{\int_T \left(\mu_o \bar{H} \cdot \bar{H}_o^* + \epsilon_o \bar{E} \cdot \bar{E}_o^* \right) d\tau} \tag{34}$$

The integral in the numerator of Eq. 34 is to be taken over the entire inner surface S of the cavity, while the integral in the denominator is taken over the volume T of the cavity.

The surface integral may be split into two parts.

$$\oint_S \bar{E} \times \bar{H}_o^* \cdot d\bar{a} = \int_{S'} \bar{E} \times \bar{H}_o^* \cdot d\bar{a} + \int_{S''} \bar{E} \times \bar{H}_o^* \cdot d\bar{a} \tag{35}$$

From section 2.3 we have

$$\bar{H} = \bar{H}_o \tag{36}$$

for large densities, and from Eq. 19 we have

$$\bar{E} = -\bar{i}_k \times \bar{H} Z_p \tag{37}$$

where $\bar{i}_k$ is the unit vector normal to the wall and pointing towards the wall. Therefore, $d\bar{a} = \bar{i}_k \, da$.

From Eqs. 36 and 37, we obtain

$$\bar{E} \times \bar{H}_o^* \cdot d\bar{a} = Z_p \left|\bar{H}_o\right|^2 da \tag{38}$$

The entire argument of section 2.3 could have been applied to a good conductor as is done by Slater.[21] Therefore, by a completely analogous argument,

$$\bar{E} \times \bar{H}_o^* \cdot d\bar{a} = Z_w \left|H_o\right|^2 da \tag{39}$$

over the conducting wall S', where Z_w is the intrinsic impedance of the conducting wall.

Upon substituting Eqs. 35, 38, and 39 in Eq. 34, we obtain

$$s - j\omega_o' = \frac{-\int_{S''} Z_p \left|\bar{H}_o\right|^2 da - \int_{S'} Z_w \left|\bar{H}_o\right|^2 da}{\int_T \left(\mu_o \left|\bar{H}_o\right|^2 + \epsilon_o \left|\bar{E}_o\right|^2\right) d\tau} \tag{40}$$

At a resonance, the total stored electric energy in a cavity is equal to the total stored magnetic energy. Therefore, Eq. 40 may be written

$$s - j\omega_o' = \frac{-\int_{S''} Z_p \left|\bar{H}_o\right|^2 da - \int_{S'} Z_w \left|\bar{H}_o\right|^2 da}{2 \int_T \mu_o \left|\bar{H}_o\right|^2 d\tau} \tag{41}$$

The resonant frequency shift of the cavity that is caused by imperfect walls is found by taking the imaginary part of Eq. 41 and is given by

$$\omega' - \omega_o' + \frac{\mathrm{Im} \int_{S'} Z_w \left|\bar{H}_o\right|^2 da}{2 \int_T \mu_o \left|\bar{H}_o\right|^2 d\tau} = - \frac{\mathrm{Im} \int_{S''} Z_p \left|\bar{H}_o\right|^2 da}{2 \int_T \mu_o \left|\bar{H}_o\right|^2 d\tau} \tag{42}$$

Let us define a frequency parameter $\delta\omega$ by

$$\delta\omega \equiv \omega' - \omega_o \equiv \omega' - \omega_o' + \frac{\mathrm{Im} \int_{S'} Z_w \left|\bar{H}_o\right|^2 da}{2 \int_T \mu_o \left|\bar{H}_o\right|^2 d\tau} \tag{43}$$

The parameter ω_o is the angular resonant frequency of the cavity which would be measured when only the plasma wall is replaced by a perfect conductor.

Upon substituting Eqs. 12 and 43 in Eq. 42, we obtain

$$\delta\omega = -\frac{c}{2} \frac{\mathrm{Im} \int_{S''} j\left[(1-j\gamma)/\eta\right]^{1/2} \left|\bar{H}_o\right|^2 da}{\int_T \left|\bar{H}_o\right|^2 d\tau} \tag{44}$$

where c is the velocity of light.

We find the change in decay time τ by taking the real part of Eq. 41; this is given by

$$\frac{1}{\tau} = \frac{\mathrm{Re}\int_{S''} Z_p \left|\bar{H}_o\right|^2 da + \mathrm{Re}\int_{S'} Z_w \left|\bar{H}_o\right|^2 da}{2\mu_o \int_T \left|\bar{H}_o\right|^2 d\tau} \tag{45}$$

Here, τ, the time constant of the decay of the fields in the cavity, is related to the internal Q and the resonant frequency of the cavity by

$$\tau = \frac{2Q}{\omega_o} \tag{46}$$

The plasma Q, or Q_p, measures the effects of plasma-power losses on the microwave characteristics of the resonant cavity and is given by

$$\frac{1}{Q_p} \equiv \frac{\mathrm{Re}\int_{S''} Z_p \left|\bar{H}_o\right|^2 da}{\omega_o \mu_o \int_T \left|\bar{H}_o\right|^2 d\tau} \tag{47}$$

and Q_o, the internal or unloaded Q of the cavity with the plasma replaced by a perfect conductor, is given by

$$\frac{1}{Q_o} \equiv \frac{\mathrm{Re}\int_{S'} Z_w \left|\bar{H}_o\right|^2 da}{\omega_o \mu_o \int_T \left|\bar{H}_o\right|^2 d\tau} \tag{48}$$

Substituting Eqs. 46-48 in Eq. 45, we obtain

$$1/Q = 1/Q_p + 1/Q_o \tag{49}$$

The plasma coupling coefficient β_p is the ratio of the power dissipated in the plasma wall to that dissipated in the conducting wall. It is defined by

$$\beta_p \equiv Q_o/Q_p \tag{50}$$

From Eqs. 12, 49, and 50, we obtain

$$\beta_p = \frac{Q_o c}{\omega_o} \frac{\mathrm{Re}\int_{S''} j[(1-j\gamma)/\eta]^{1/2} \left|\bar{H}_o\right|^2 da}{\int_T \left|\bar{H}_o\right|^2 d\tau} \tag{51}$$

Equations 44 and 51 relate the normalized electron density and the normalized collision frequency to the frequency shift $\delta\omega$ caused by the plasma wall and to the plasma coupling coefficient β_p. If the integrals of Eqs. 44 and 51 can be evaluated, the electron density and collision frequency can be expressed in terms of β_p, $\delta\omega$, Q_o, and ω_o. The parameters Q_o and ω_o are not dependent on the properties of the plasma wall and can be measured by standard techniques. In the following sections, we shall consider methods of measuring β_p and $\delta\omega$.

It is interesting to note that, if γ is independent of position, the collision frequency ν_c may be obtained without knowledge of either the fields inside the cavity or the electron density distribution along the boundary of the plasma wall. Dividing Eq. 44 by Eq. 51, we obtain

$$\frac{\delta\omega}{\beta_p} = -\frac{\omega_o}{2Q_o}\,\frac{1+(1+\gamma^2)^{1/2}}{\gamma} \tag{52}$$

or

$$\gamma = \frac{\nu_c}{\omega_o} = \frac{-4\beta_p Q_o \delta\omega/\omega_o}{(2Q_o\delta\omega/\omega_o)^2 - \beta_p^2} \tag{53}$$

In order to evaluate the integrals which appear in Eqs. 44 and 51, we define an averaged density parameter η_a by

$$\eta_a \equiv \left[\frac{\int_{S''} \left|\bar{H}_o\right|^2 da}{\int_{S''} (\eta)^{-1/2} \left|\bar{H}_o\right|^2 da}\right]^2 \tag{54}$$

If the electron density is independent of position over the surface of the plasma wall, then η_a reduces to the correct value.

Combining the definition contained in Eq. 54 with Eqs. 44 and 51, we obtain

$$\delta\omega = -\frac{c}{2}\,\frac{K_g}{(\eta_a)^{1/2}}\,\mathrm{Im}\left[j(1-j\gamma)^{1/2}\right] \tag{55}$$

and

$$\beta_p = \frac{Q_o c}{\omega_o}\,\frac{K_g}{(\eta_a)^{1/2}}\,\mathrm{Re}\left[j(1-j\gamma)^{1/2}\right] \tag{56}$$

where K_g is a geometrical constant and is given by

$$K_g = \frac{\int_{S''} \left|\bar{H}_o\right|^2 da}{\int_T \left|\bar{H}_o\right|^2 d\tau} \tag{57}$$

Using the definitions of η_a and γ given in Eqs. 4 and 5, we can write Eqs. 55 and 56 in alternative form so that we obtain

$$\frac{\delta\omega}{\omega_o} = -\frac{cK_g}{2\omega_p} \mathrm{Im}\left[j(1-j\nu_c/\omega_o)^{1/2}\right] \tag{58}$$

and

$$\beta_p = \frac{Q_o cK_g}{\omega_p} \mathrm{Re}\left[j(1-j\nu_c/\omega_o)^{1/2}\right] \tag{59}$$

The plasma frequency ω_p is now a geometrically averaged plasma frequency and can be expressed in terms of the true plasma frequency with the aid of Eqs. 4 and 54.

The above equations can be solved for the average density n_a and the collision frequency ν_c in terms of the parameters of the equivalent circuit. The results are

$$\nu_c = \frac{-4\delta\omega\beta_p/Q_o}{(2\delta\omega/\omega_o)^2 - (\beta_p/Q_o)^2} \tag{60}$$

and

$$n_a = \frac{m\epsilon_o}{e^2} \frac{c^2K_g^2}{(2\delta\omega/\omega_o)^2 - (\beta_p/Q_o)^2} \tag{61}$$

2.5 THE EQUIVALENT CIRCUIT FOR A DENSE PLASMA IN A RESONANT CAVITY

A microwave cavity has an infinite number of resonant frequencies. Consequently, an exact equivalent circuit for such a device is very complicated. Beringer[22] has shown that the equivalent circuit of a cavity which joins two matched transmission lines can be simplified to the circuit of Fig. 3(a) at frequencies near a single resonance. The parallel elements represent the resonance of interest and the series term Y_s accounts for the effects of all the off-resonant cavity modes. If the reference plane in line 1 is chosen to be the point of a voltage minimum when the cavity is detuned, Y_s is pure real. This reference plane is called the "plane of the detuned short" and is the plane we shall take as our reference.

If the wall of the cavity is partly a good conductor and partly a dense plasma, the parallel-loss term G is composed of a part G_o as a result of the loss in the conductor wall and a part G_p as a result of loss in the plasma wall. We have

$$G = G_o + G_p \tag{62}$$

Similarly, the plasma loads all the off-resonant modes and we have

$$\mathrm{Re}\,(Y_s) = G_s = \frac{G_{os}G_{ps}}{G_{os} + G_{ps}} \tag{63}$$

where G_{ps} is the contribution to the series term which results from loss in the plasma wall. Thus, G_o and G_{os} are, respectively, the parallel conductance and the series conductance of the equivalent circuit when the volume occupied by the plasma is replaced by a perfect conductor.

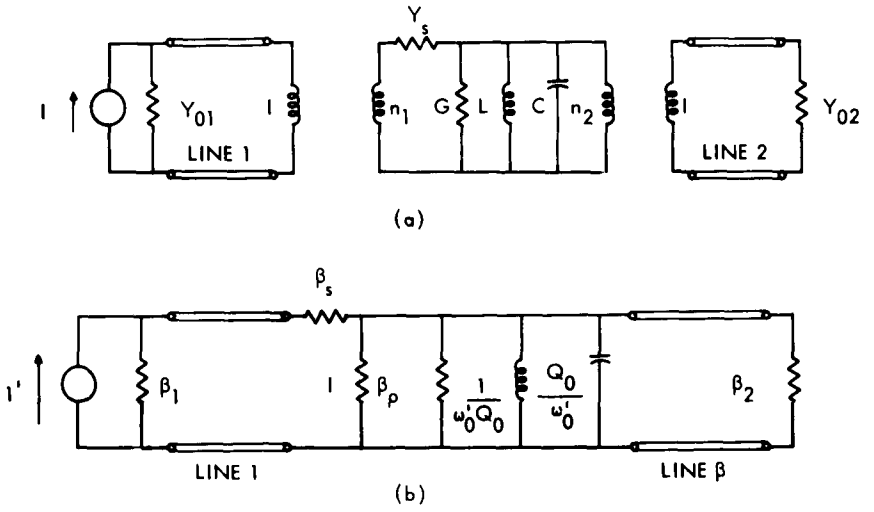

Fig. 3. (a) Cavity equivalent circuit joining two transmission lines.
(b) Normalized equivalent circuit.

The resonant frequency ω'_o of the system is the cavity resonant frequency ω_o with the plasma perfectly conducting, plus the frequency shift $\delta\omega$ caused by the plasma and is given by

$$\omega'_o = \omega_o + \delta\omega \tag{64}$$

The formula for $\delta\omega$ is given by Eq. 43.

The unloaded Q_o of the cavity with the plasma replaced by a perfect conductor is given by

$$Q_o = \frac{\omega_o C}{G_o} \tag{65}$$

It is convenient to define a number of parameters by the following equations:

$$\beta_1 = \frac{Y_{o1}}{n_1^2 G_o} \tag{66}$$

$$\beta_2 = \frac{Y_{o2}}{n_2^2 G_o} \tag{67}$$

$$\beta_s = G_s/G_o \tag{68}$$

$$\beta_p = G_p/G_o \tag{69}$$

and

$$\Delta\omega = \omega - \omega_o \tag{70}$$

where β_1 and β_2 are, respectively, the input and output coupling coefficients; β_s is a measure of the loss in the off-resonant cavity modes compared to that in the resonant mode; β_p is the plasma coupling coefficient which was defined in Eq. 50; and $\Delta\omega$ is the difference between the driving frequency ω and the system resonant frequency ω_o with the plasma replaced by a perfect conductor.

We shall be interested in measuring the parameters β_p and $\delta\omega$ and the distribution of microwave power to various portions of the circuit. Therefore, the circuit of Fig. 3(b) will be used in place of the circuit of Fig. 3(a). The second circuit is obtained from the first by transforming all the elements through the ideal transformers into the cavity and dividing by G_o. The circuit of Fig. 3(b) is convenient to use because the circuit parameters are easily measured by standard techniques. This circuit does not retain the proportionality between the voltages in lines 1 and 2 which exists in the circuit of Fig. 3(a). However, the values of these voltages are not of interest.

The series term β_s is much larger than unity if the cavity is not greatly overcoupled to line 1 or line 2. Therefore, we shall assume that β_s is infinite, in which case it can be replaced by a short circuit. The conditions under which this assumption is valid can be found by calculating the distribution of the microwave power dissipated in the circuit of Fig. 3(b).

The real power P_a absorbed by the cavity is given, in terms of the incident power P_i and the reflection coefficient Γ, by

$$P_a = (1-|\Gamma|^2)\, P_i \tag{71}$$

where Γ is related to the admittance Y the cavity presents to line 1 by

$$\Gamma = \frac{\beta_1 - Y}{\beta_1 + Y} \tag{72}$$

From Fig. 3(b) we find that Y is the admittance looking into plane A - A' and is given by

$$Y = \frac{\beta_s[1+\beta_2+\beta_p+jQ_o(\omega/\omega'_o-\omega'_o/\omega)]}{1+\beta_s+\beta_2+\beta_p+jQ_o(\omega/\omega'_o-\omega'_o/\omega)} \tag{73}$$

At frequencies near the resonant frequency of the system, with the aid of Eqs. 64 and 70, we obtain

$$Q_o\left[\frac{\omega}{\omega'_o}-\frac{\omega'_o}{\omega_o}\right] \simeq 2Q_o\frac{\Delta\omega-\delta\omega}{\omega_o} \tag{74}$$

If we let

$$b = 2Q_o\frac{\Delta\omega-\delta\omega}{\omega_o} \tag{75}$$

and

$$g = 1+\beta_2+\beta_p \tag{76}$$

and substitute Eqs. 72-76 in Eq. 71, we obtain

$$\frac{P_a}{P_i} = \frac{4g\beta_1}{b^2+[g+\beta_1/(1+\beta_1/\beta_s)]^2}\left\{1+\frac{g}{\beta_s}\left[1+\left(\frac{b}{g}\right)^2\right]\right\} \tag{77}$$

It can be shown that $\frac{g}{\beta_s}\left[1+\left(\frac{b}{g}\right)^2\right]$ is the ratio of the power dissipated in the series element β_s to the total power dissipated in g. This term will be small when both g and b are small, that is, when the electron density of the plasma is large and the system is excited very near resonance. Under these conditions, β_s may be assumed infinite and Eq. 77 reduces to

$$\frac{P_a}{P_i} = \frac{4g\beta_1}{b^2+[g+\beta_1]^2} \tag{78}$$

2.6 THE MEASUREMENT OF β_p AND $\delta\omega$

In section 2.4 it was shown that the collision frequency and a geometrically averaged electron density of a plasma in a resonant cavity can be calculated from measurements of β_p and $\delta\omega$. Several methods of measuring these parameters have been given previously.[8-11] In this section, two methods of measuring β_p and $\delta\omega$, which were found to be useful, are described.

a. Microwave Energy Used as a Probe

If the plasma is not produced by the microwave energy and the probing power is sufficiently small, the parameters of the discharge are independent of the microwave energy. With this assumption, it is possible to determine β_p/Q_o and $\delta\omega$ by measuring

the resonant frequency of the system and the standing-wave ratio at resonance, both with the plasma present and with the plasma replaced by a good conductor. Inspection of Eqs. 60 and 61 shows that knowledge of β_p/Q_o and $\delta\omega$ is sufficient to determine the collision frequency and the electron density of the plasma.

The resonant frequency ω_o of the cavity with the plasma replaced by a perfect conductor is found by measuring the cavity resonant frequency with a good conductor replacing the plasma and then adding to it the calculated shift in resonant frequency as a result of the good conductor. This calculation is described in the Appendix. We then find $\delta\omega$ by subtracting ω_o from the measured cavity resonant frequency with the plasma present.

We find β_p/Q_o by the following procedures: Let

$$\rho_o = \frac{1 + \beta_2 + \beta_m}{\beta_1} \tag{79}$$

and

$$\rho_p = \frac{1 + \beta_2 + \beta_p}{\beta_1} \tag{80}$$

where β_m is the ratio of the power dissipated in conductor which replaces the plasma to the power dissipated in the remainder of the cavity wall and may be defined by

$$\beta_m = \frac{Q_o}{Q_m} \tag{81}$$

where Q_m is the contribution to the unloaded Q of the cavity resulting from the conductor that replaces the plasma. From Fig. 3(b), we see that ρ_o is the VSWR at resonance with the conductor that replaces the plasma present if the cavity is overcoupled, and ρ_o is the reciprocal of the VSWR at resonance if the cavity is undercoupled. Similarly, ρ_p is the VSWR at resonance with the plasma present if the cavity is overcoupled. The unloaded Q_o with the plasma replaced by a perfect conductor may be expressed in terms of the loaded Q_ℓ, the input and output coefficients, and β_m as

$$Q_o = (1+\beta_1+\beta_2+\beta_m)\, Q_\ell \tag{82}$$

Solving Eqs. 79-82 for β_p/Q_o, we obtain

$$\frac{\beta_p}{Q_o} = \frac{1}{Q_m} + \frac{\rho_p - \rho_o}{(\rho_o+1)\, Q_\ell} \tag{83}$$

Notice that it is not necessary to know β_1 or β_2 to calculate β_p/Q_o. Thus, β_p/Q_o can be calculated from measurements of the loaded Q and of the VSWR at resonance with the plasma present and also with a good conductor replacing the plasma. A perturbation technique that is described in the Appendix is used to calculate Q_m. It

is also necessary to know whether the cavity is overcoupled or undercoupled to line 1 in each case. This is easily determined by comparing the positions of the voltage minima on line 1 at resonance and when the cavity is detuned from resonance. If the two positions coincide, the cavity is undercoupled and the reciprocal of the measured VSWR should be substituted for ρ in Eqs. 79 and 80. If the detuned position of the voltage minimum coincides with the position of the voltage maximum in line 1 at resonance, the cavity is overcoupled and ρ is the measured VSWR.

b. Plasma Produced by the Microwave Energy

If the plasma is produced by the microwave energy, the technique previously described cannot be used because it is impossible to excite the system at its resonant frequency. The resonant frequency of the system depends on the parameters of the plasma which, in turn, depend, among other things, on the amount of microwave power dissipated in the plasma. Since the amount of power coupled into the cavity from the microwave source depends on the resonant frequency of the system, the parameters of the system are all interrelated. These relations must be simultaneously satisfied for the system to operate in a steady state. In general, all conditions cannot be satisfied if the system resonant frequency and the applied frequency are equal.

We can calculate $\delta\omega$ and β_p by measuring the VSWR in line 1 and the ratio of the power P_t transmitted through the cavity to the incident power P_i as well as the frequency of the applied microwave energy.

From Fig. 3(b), we obtain, upon neglecting β_s,

$$P_t = \frac{P_a \beta_2}{1 + \beta_2 + \beta_p} \tag{84}$$

where P_a is the power coupled into the cavity from line 1. Solving for β_p, we obtain

$$\beta_p = \beta_2 \left[\frac{P_a}{P_t} - 1 \right] - 1 \tag{85}$$

or, if ρ is the VSWR in line 1 at the applied frequency, we find

$$\beta_p = \beta_2 \left[\frac{4\rho}{(1+\rho)^2} \frac{P_i}{P_t} - 1 \right] - 1 \tag{86}$$

From Eqs. 75, 76, and 78, we see that $\delta\omega$ is given by

$$\delta\omega = \Delta\omega = \frac{\omega_o}{2Q_o} \left[4\beta_1\beta_2 P_i / P_t - (1+\beta_1+\beta_2+\beta_p)^2 \right]^{1/2} \tag{87}$$

We shall also wish to know the power absorbed in the plasma P_p. From Fig. 3(b) we can see that P_p is related to the transmitted power by

$$P_p = \frac{\beta_p}{\beta_2} P_t \tag{88}$$

It should be remembered that β_s was assumed infinite in the development of these relations. This is liable to be a bad assumption because the system is not at resonance. Thus, it is expected that this technique will give results that are less accurate than those obtained by the technique of using microwave energy as a low-level probe.

III. EXPERIMENTAL EQUIPMENT, OBSERVATIONS, AND RESULTS

3.1 INTRODUCTION

The plasma studied in these experiments was formed by the ionization of helium at pressures of 0.5-8.0 mm Hg.

The plasma was produced in a quartz tube that lay along the axis of a cylindrical resonant cavity by the fields of the TE_{111} coaxial mode. The plasma served as the center conductor for this mode. This mode was excited by a 10-μsec pulse of 10-cm microwave energy generated by a QK327 magnetron. The TE_{011} coaxial mode that falls in the 6-cm band was used as a low-level probe to measure the properties of the plasma.

The transient behavior of the system is discussed. The electron density of the plasma increased very rapidly with each microwave pulse and appeared to reach a constant value before the microwave pulse was extinguished. It was found that under certain conditions the system operates in two states during a single pulse.

The stable points at which the system can operate are calculated on the basis of the theory of Section II and the results of electron-density measurements. The steady-state behavior of the system can be explained on the basis of the results of the operating-point analysis.

The microwave characteristics of the system are discussed, and experimental data are given. The amount of power that can be coupled into the plasma is limited by breakdown of the gas between the quartz tube and the metal cavity wall.

Measurements of the electron density of the plasma are reported. Electron densities calculated from measurements of both the 10-cm-band and 6-cm-band parameters are compared with the peak microwave power dissipated in the plasma. The 6-cm-band calculations indicate that the plasma electron density is linearly related to the power dissipated in the discharge. The maximum electron densities measured by the probing mode are about $2 \times 10^{14}/cm^3$ at an expenditure of 80 kw of peak power in the discharge.

Measurements of the electron collision frequency of the plasma are reported and compared with the value of collision frequency given by Brown.[23] The measured collision frequencies are in reasonable agreement with Brown's values.

The light generated by the discharge was studied visually and with the aid of a phototube and an oscilloscope. The discharge is brightest in a thin shell that is distributed over the plasma surface. The spectral distribution of the light was studied with a monochrometer. Silicon and oxygen lines, as well as helium lines, were detected.

3.2 EXPERIMENTAL APPARATUS AND TECHNIQUES

a. The Vacuum System

The quartz tube containing the plasma was connected to a glass vacuum system that could be evacuated to less than 10^{-7} mm Hg. A block diagram of the vacuum system

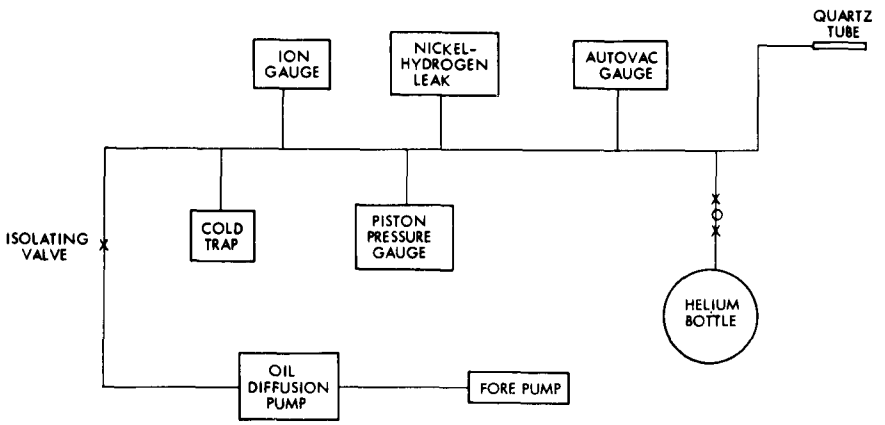

Fig. 4. Vacuum system.

appears in Fig. 4. A portion of the vacuum system, including the quartz tube, could be isolated from the pumps. The isolated vacuum system would hold a pressure of less than 10^{-5} mm Hg for several hours; and it could be filled with helium from a bottle of spectroscopically pure helium (impurities of less than one part in 10^4). Hydrogen could also be admitted into the isolated vacuum system by diffusion through a heated nickel leak.

Neutral-gas pressures were measured with three vacuum gauges. Very low pressures were measured with an ion gauge of the Bayard-Alpert type; pressures from 10^{-3}-8 mm Hg, with an Autovac thermocouple gauge; and pressures from 0.5-200 mm Hg, with a piston pressure gauge.[24] The pressures measured with the Autovac gauge and the piston gauge were believed to be accurate to within 15 per cent.

b. The Resonant Cavity

The resonant cavity and the quartz tube that contains the discharge are shown in Fig. 5. The picture also shows the methods that are used to couple the cavity to the remainder of the microwave system. This configuration was chosen to minimize the coupling of the low-power probing mode to the waveguide that carries the high-power microwave energy.

The fields of the TE_{111} coaxial cavity mode were used to produce the discharge. The plasma served as the center conductor of this mode. Microwave energy coupled to the cavity from a 10-cm (S-band) waveguide system was used to excite this mode. The plasma produced by the S-band power was probed with the TE_{011} coaxial mode, which is resonant in the 8-cm band or C-band. The smaller waveguide in Fig. 5 is connected to the C-band equipment.

The TE_{011} mode is degenerate with the TM_{111} mode. This degeneracy was removed by the quartz tube and the iris coupling holes, but the TM_{111} resonance still occurred near enough to the TE_{011} resonance to confuse the experiments. A brass plug (see

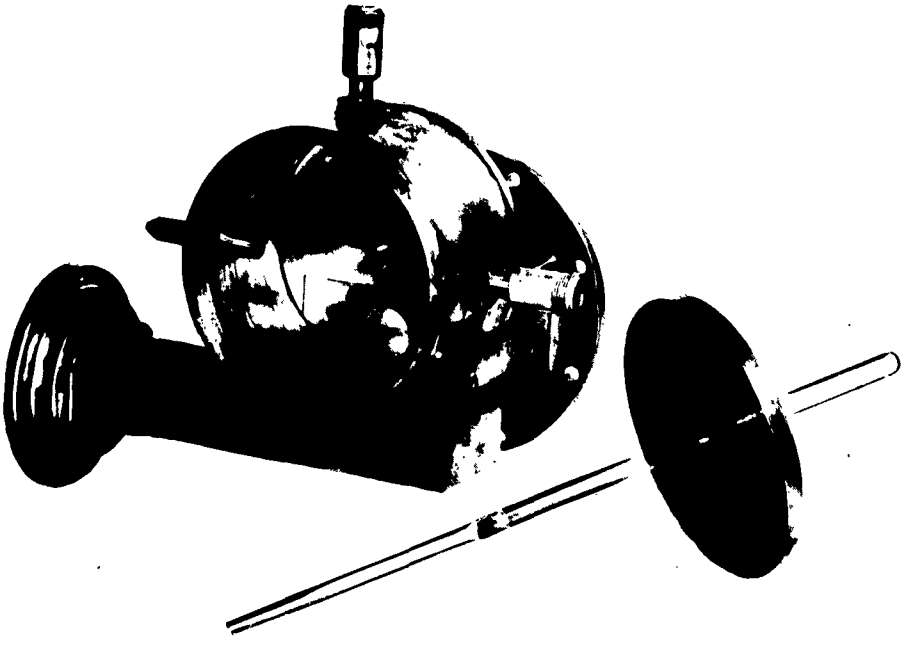

Fig. 5. Resonant cavity.

Fig. 5) was inserted into the wall of the cavity to further split the two modes. The plug lowered the resonant frequency of the TM_{111} over 100 mc and increased the resonant frequency of the TE_{011} mode about 1 or 2 mc; it also removed the polarization degeneracy of the TE_{111} mode.

A coaxial probe and coupling loop were used to sample the fields of the TE_{111} mode. The coupling coefficient of the probe is denoted by β_3 and the loop coupling coefficient is β_2.

Table I. Cavity parameters at SF_6 pressure of 10 psig.[a]

Coaxial TE_{111} Mode		Coaxial TE_{011} Mode	
f_o	2732.0 mc	f_o	4225.9 mc
Q_o	7020.0	Q_l	2490.0
β_1	2.53	ρ_o	1.11 overcoupled
β_2	0.181	K_g	0.115/cm
β_3	0.02		
β_s	250.0		
K_g	0.096/cm		

[a]Cavity i.d., 10.273 cm; length, 6.853 cm. Quartz tube i.d., 0.9 cm; o.d., 1.1 cm.

Table I lists the physical dimensions of the cavity, of the quartz tube and the microwave parameters of the TE_{111} and TE_{011} coaxial cavity modes. The experimental techniques used to measure the microwave parameters of the cavity are described in the Appendix.

A small window was placed in the cavity wall so that the light generated by the discharge could be observed. The window, on the right side of the cavity between the coupling loop and the C-band guide, is shown in Fig. 5.

The resonant cavity was pressurized with sulfur hexafluoride (SF_6) in an attempt to prevent breakdown from occurring in the volume between the quartz tube and the cavity walls. This pressure was held at 10 psig for all experiments. It was found to be impossible to prevent the SF_6 from breaking down when the cavity was excited with high incident-power levels at frequencies just below 2732 mc. The SF_6 breakdown occurred along a diagonal at the cavity center from top to bottom. This is the position at which the electric field of the coaxial TE_{111} mode is at a maximum. Since x-radiation is produced in the cavity when the SF_6 is broken down, the breakdown was not studied in any detail.

c. The S-Band Equipment

Figure 6 is a block diagram of the S-band equipment used in this experiment, and the apparatus itself is shown in Fig. 7.

The microwave energy used to produce the plasma was generated by a Raytheon QK327 magnetron that was tunable from 2696 to 2816 mc. The magnetron generated a peak power of approximately 800 kw which was found to be adequate for the experiments of this report. The magnetron was modulated by a 10-μsec pulse, at a rate of 60 pulses each second. Thus, the duty factor was 6×10^{-4}. Figure 8 shows oscillograms of

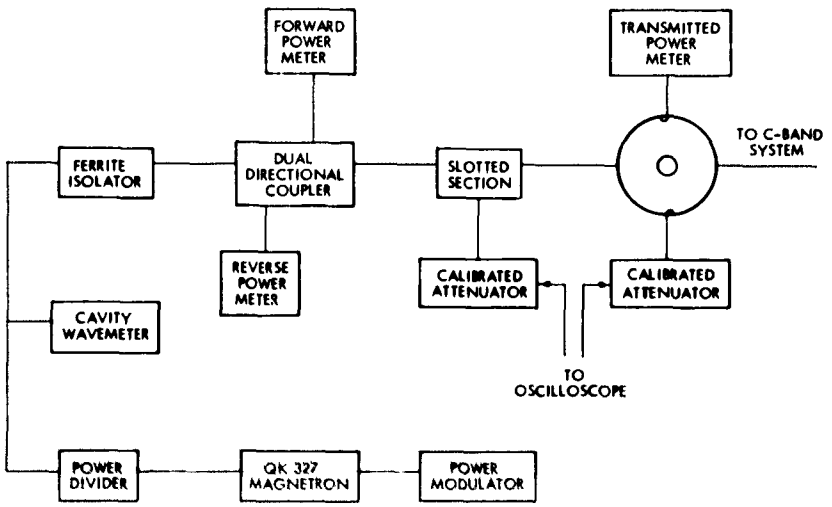

Fig. 6. S-band system.

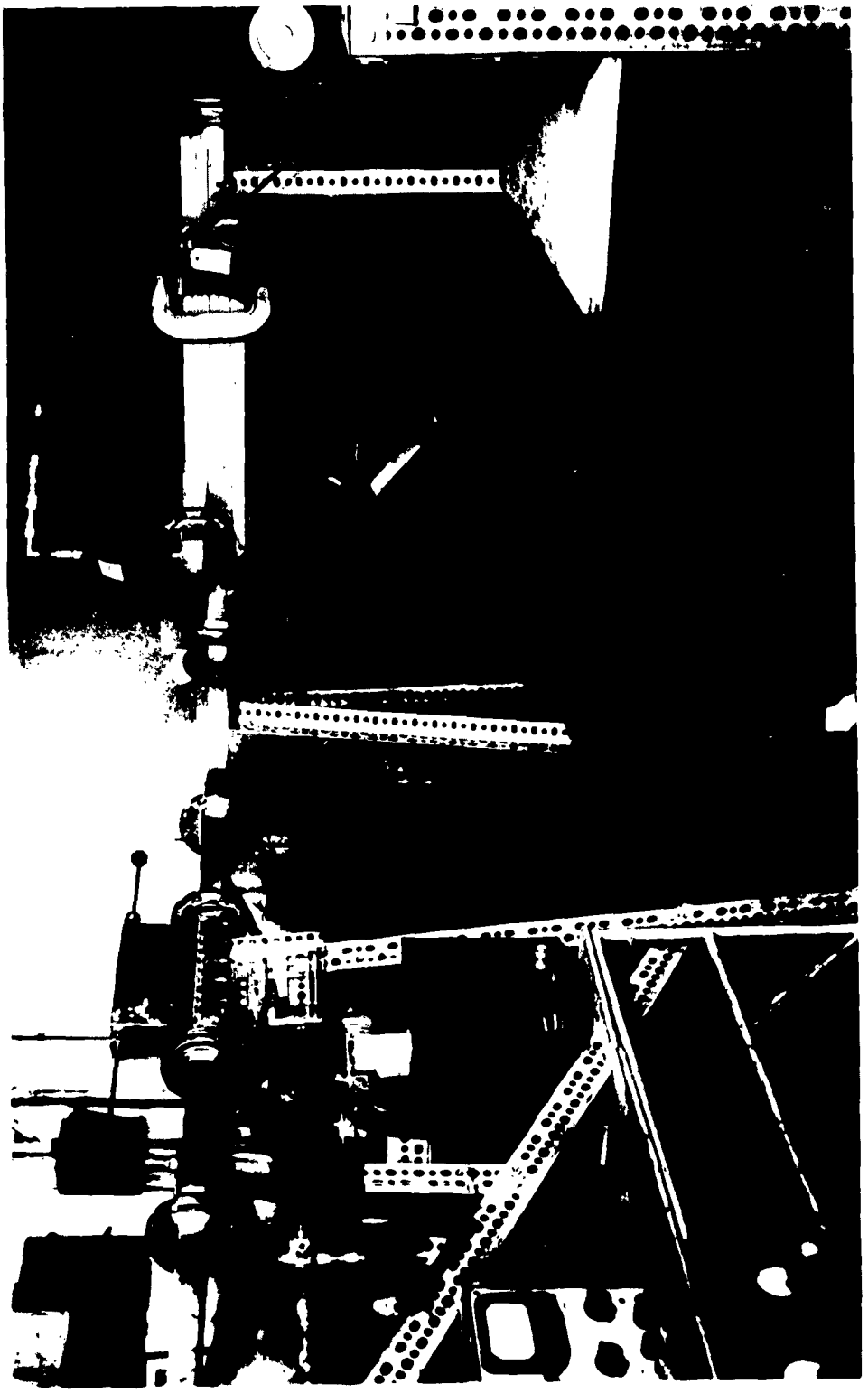

Fig. 7. S-band equipment.

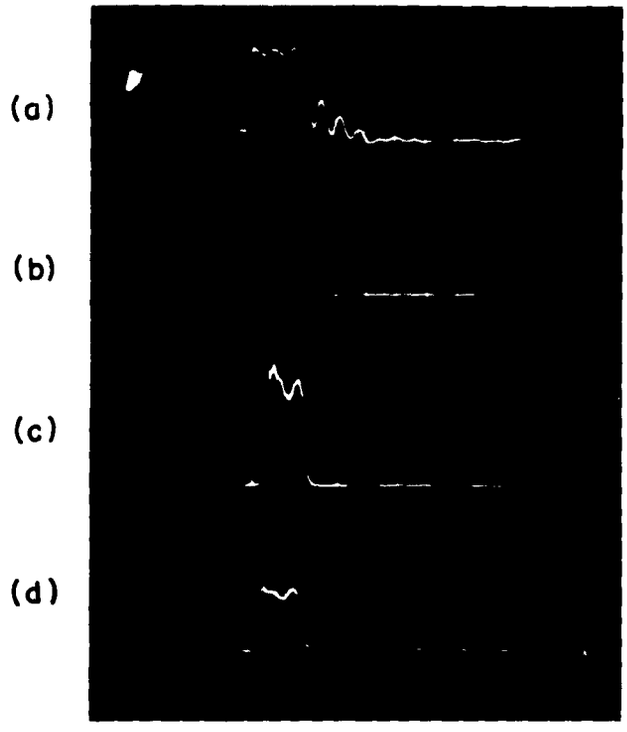

Fig. 8. Oscillograms of (a) the current pulse applied to the magnetron; (b) the resulting microwave pulse; (c) the magnitude of the field within the cavity, showing a transition at $\tau = 3$ μsec; and (d) the light generated by a 0.5-mm discharge. The time scale is 5 μsec/cm.

(a) the current pulse applied to the magnetron and (b) the resulting microwave pulse. The ripple in the current pulse caused both amplitude and frequency modulations of the microwave energy which account for the ripple that can be seen in the first 10 μsec of the oscillograms of Figs. 8, 24, and 25.

The level of the microwave energy incident upon the cavity was controlled by a waveguide power divider of the type described by Teeter and Bushore.[25] The peak incident power could be varied from the 800 kw generated by the magnetron to less than 80 watts with the use of this device.

The magnetron was isolated from the load by two Raytheon ferrite isolators that provided a total isolation of over 20 db, and insured that the cavity appeared to be excited by a matched generator as required by the theory of Section II. These isolators were water-cooled and were capable of absorbing all the power generated by the magnetron.

The incident and reflected power in the S-band guide were sampled by a 20-db dual-directional coupler with a directivity of more than 40 db. The power coupled from the waveguide was attenuated by calibrated coaxial attenuators and measured by two Hewlett-Packard Model 430 C power meters.

The standing-wave ratio in the S-band waveguide was measured with the aid of a

waveguide slotted section. The energy coupled from the waveguide by the slotted section probe was transmitted by coaxial cable to an adjustable waveguide sliding-vane attenuator that had previously been calibrated. The level of the microwave energy that passed through the attenuator was detected by a crystal diode and displayed on a Tektronix 545 A oscilloscope. The standing-wave ratio in the S-band guide was measured by observations of the attenuator settings that result in equal deflections on the oscilloscope when the slotted section probe was at a voltage maximum and at a voltage minimum. Standing-wave ratios as large as 40 db could be measured by this method. Unfortunately, errors as large as 2 db were noted when measurements of standing-wave ratios above 30 db were attempted. These errors were principally caused by the inaccurate placing of the slotted section probe on the true voltage minimum in the S-band waveguide. Also, because of the amplitude and frequency modulation of the microwave pulse, the position of the voltage minimum was difficult to recognize. The last item on the S-band waveguide line is the resonant cavity that was discussed in section b above.

The entire S-band waveguide system was pressurized with air at 15 psig to prevent breakdown. The waveguide pressure system was separated from the cavity pressure system by a mica window placed in the S-band guide at the waveguide joint nearest the cavity.

Microwave energy coupled out of the cavity by the coupling loop was attenuated and measured by a Hewlett-Packard power meter. The power coupled from the cavity by the coupling probe was fed through a calibrated, adjustable, waveguide attenuator, was detected, and was displayed on a Tektronix 545 A oscilloscope. The attenuator setting and oscilloscope deflection were recorded and compared with the microwave power measured by the power meter. This procedure calibrated the probe circuits for absolute power measurements. Notice that the power measured by observations of the oscilloscope deflection and the setting of the calibrated attenuators was actually the power dissipated in the power-meter circuit.

The above method has the advantage of permitting the instantaneous power transmitted through the cavity to be measured as a function of time. This measurement was found to be necessary for reasons pointed out in section 3.3.

A high-Q cavity wavemeter or "Echo Box," Model TS-270/UP, was used to measure the frequency of the S-band energy.

d. The C-Band Equipment and Techniques

The C-band equipment used in these experiments is pictured in Fig. 9, and Fig. 10 shows a block diagram of the system. This equipment was used to measure the resonant frequency and the standing-wave ratio at the resonance of the TE_{011} cavity mode with the coaxial plasma. From these measurements, the averaged electron density and collision frequency of the plasma center conductor were calculated on the basis of the theory presented in Section II and the data contained in Table I.

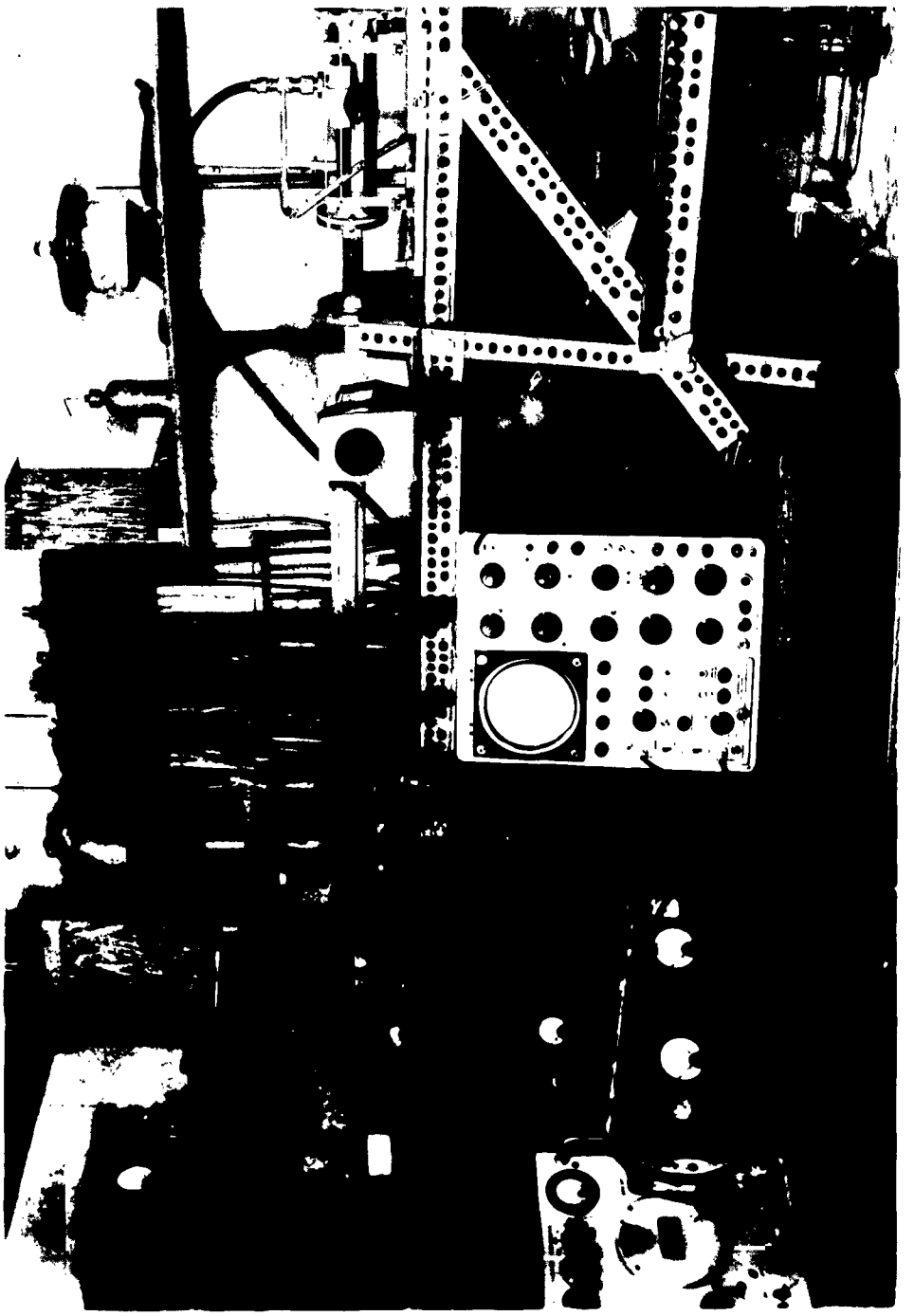

Fig. 9. C-band equipment.

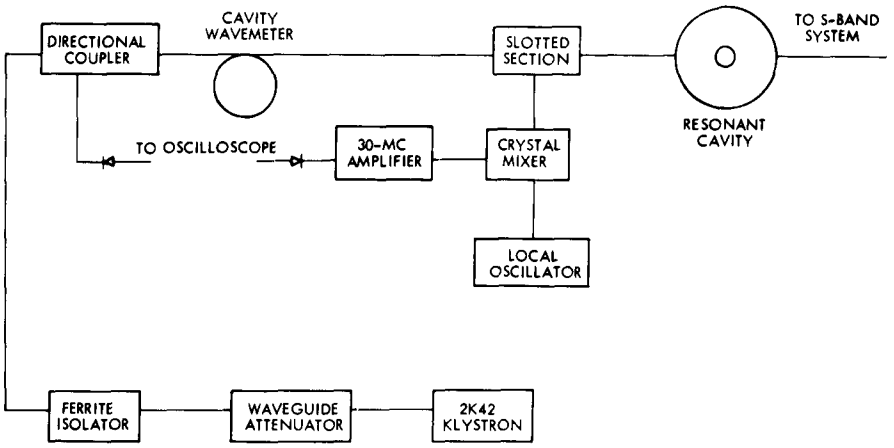

Fig. 10. C-band system.

The C-band energy was generated by a 2K42 klystron that is tunable from approximately 4050 to 4350 mc and that generates a maximum power of less than 250 mw. Since this is more than 50 db below the level of the S-band power, the C-band energy was assumed to produce a negligible effect on the parameters of the discharge.

A 10-db waveguide directional coupler placed so as to monitor the power reflected by the cavity was used to detect the resonance of the TE_{011} coaxial mode.

The VSWR in the C-band guide was measured with a waveguide slotted section and a microwave receiver composed of a local oscillator and a high-gain 30-mc amplifier. Only when the cavity was observed to be resonant at the excitation frequency were VSWR measurements made.

Because the discharge is produced by each pulse of S-band energy, the resonant frequency of the TE_{011} mode changes with time. The nature of this change can be explained with the use of the diagram contained in Fig. 12.

Figure 11 is a sketch of the electron density within the quartz tube as a function of time. At t = 0, the S-band power is applied, which causes the electron density to rise to its steady-state value n_o. Ten μsec later, the S-band power is removed and the

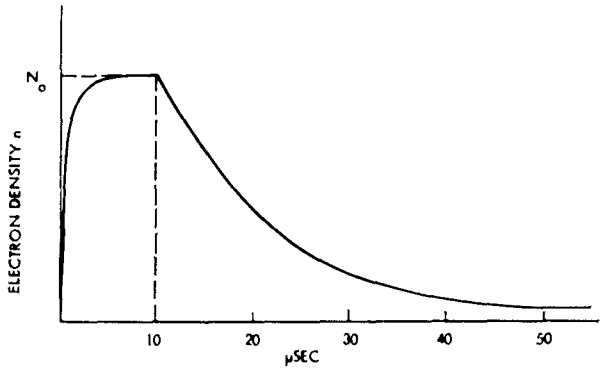

Fig. 11. Plasma electron density as a function of time.

electron density decays toward zero. The rate at which the density decays depends on the electron-loss processes in the quartz tube. According to Eq. 55, the resonant frequency of the cavity varies inversely as the square root of the electron density. Therefore the resonant frequency of the cavity varies with time in the manner sketched in Fig. 12.

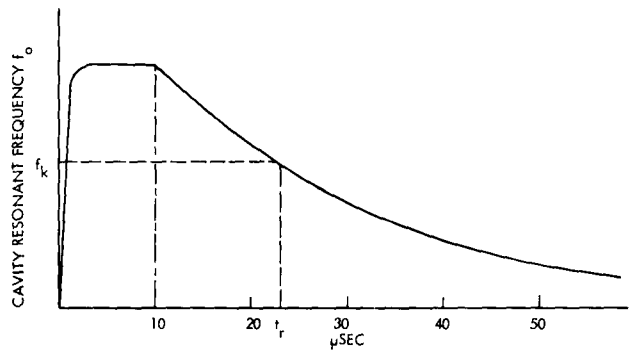

Fig. 12. The TE_{011} coaxial-mode resonance as a function of time, showing a resonance observed at time t_r produced by a klystron at frequency f_k.

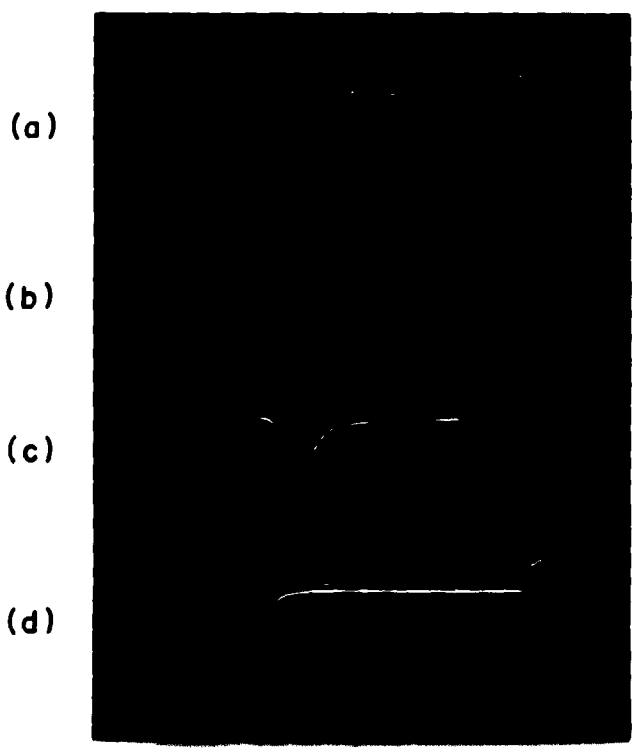

Fig. 13. Oscillograms of the C-band power reflected by the cavity at frequencies: (a) 4167.5; (b) 4180; (c) 4202; and (d) 4215 mc. Time scale is 20 μsec/cm.

Let us assume that the C-band klystron is tuned to the frequency ω. At $t = t_r$ the resonant frequency of the cavity ω_o will equal the frequency of the C-band klystron and, if the power reflected by the cavity is displayed on an oscilloscope, a resonance will be observed. Figure 13 is an oscillogram of the reflected C-band power versus time, showing the types of waveforms observed. If a measurement of the resonant frequency of this mode with a perfect conductor replacing the plasma is subtracted from a measurement of the klystron frequency, the resulting shift in the resonant frequency ($\delta\omega$) of the mode (because the plasma is not a perfect conductor) is found at time t_r. Adjusting the frequency of the C-band klystron toward higher frequencies will cause the time t_r at which a resonance is observed to become less until it is in the region in which the electron density is not changing with time ($t_r < 10$ μsec).

In the C-band experiments, the procedure outlined above was used to measure the frequency shift caused by the plasma. The standing-wave ratio in the C-band guide was then measured at the time a resonance was observed. These measurements were performed only when the frequency of the C-band klystron was adjusted, so that the TE_{011} resonance was observed to occur during the S-band pulse.

3.3 SYSTEM OPERATION

The plasma in the quartz tube was produced by each pulse of microwave energy. Under certain conditions, the system appears to reach a steady state before the microwave pulse is extinguished (10 μsec). In this section, we shall consider the transient buildup of the discharge with each pulse and the conditions which must be fulfilled for steady-state operation of the system.

a. Transient Buildup

Equation 55 indicates that as the electron density of the plasma center conductor increases, the resonant frequency of the cavity approaches 2732 mc from lower frequencies. Therefore, when microwave power is applied to the plasma, the electron density will increase to a point at which the energy required to maintain the discharge is just that supplied by the microwave energy. The time required for the electron density of the discharge to reach a constant value depends on how much larger the available microwave power is than that required to maintain the discharge. (See, for instance, Madan, Gordon, Buchsbaum and Brown.[18])

At applied frequencies slightly less than 2732 mc, the discharge would operate in what appeared to be two stable states. The existence of two states was recognized by observations of the standing-wave ratio in the S-band guide or of the magnitude of the field within the cavity as a function of time.

Figure 14 is a sketch of the magnitude of the electromagnetic field within the cavity versus time, as observed on a high-speed oscilloscope. The sketch shows the two states of operation and a transition occurring from the lower state 1 to the upper state 2 at

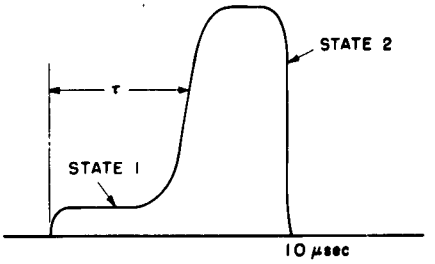

Fig. 14. The wave shape of the microwave-field intensity inside the cavity as a function of time, showing a transition from state 1 to state 2 at τ seconds.

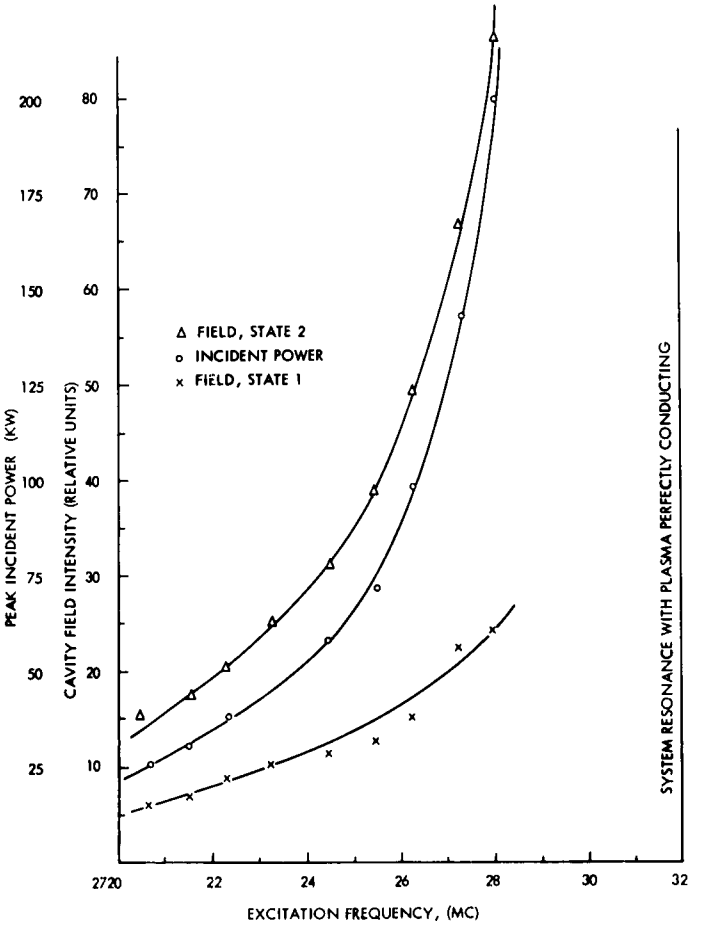

Fig. 15. Cavity-field intensity and incident power as functions of the excitation frequency, for the transition time τ of 6 μsec with the helium discharge at 0.92 mm Hg.

time τ. At low values of incident power, the discharge operates in state 1. As the incident power is increased, a transition from state 1 to state 2 is observed at the end of the pulse; it shifts smoothly toward the beginning of the pulse as the incident power is increased. When the discharge is operating in the second state, the magnitude of

the field within the cavity increases only slightly with increasing incident power.

The time (τ) at which the transition occurs and the incident power necessary to initiate the transition are strong functions of the frequency of the microwave energy. Figure 15 is a plot of the incident microwave power and the relative fields of both states inside the cavity versus the frequency of the microwave energy. In this plot, the time (τ) at which the transition occurred was held at 6 μsec. The gas used was helium at a pressure of 0.92 mm Hg. It was impossible to obtain points nearer 2732 mc because the microwave field of state 2 became large enough to break down the SF_6 inside the cavity.

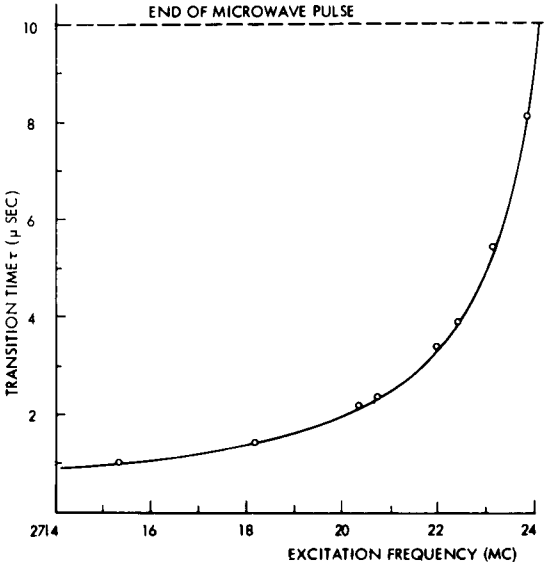

Fig. 16. Variation of transition time τ with excitation frequency at 100 kw incident power. The helium discharge is at a pressure of 0.5 mm Hg.

Figure 16 shows the variation of the transition time τ with the excitation frequency when the incident power is held constant. These data were taken on a helium discharge at a gas pressure of 0.5 mm Hg. The incident microwave power was 100 kw.

b. Steady-State Operation

The conditions for steady-state operation can be found by equating the power coupled into the plasma to the power that the plasma requires to operate at a density n.

In Section II, it was shown that the power coupled into the cavity from the microwave source is given in terms of the incident power and the cavity parameters by

$$\frac{P_a}{P_i} = \frac{4\beta_1(1+\beta_2+\beta_p)}{(1+\beta_1+\beta_2+\beta_p)^2 + [2Q_o(\Delta\omega-\delta\omega)/\omega_o]^2} \tag{89}$$

where we have neglected the series element in the equivalent circuit of Fig. 3(b). From Fig. 3(b), we have

$$\frac{P_p}{P_a} = \frac{\beta_p}{(1+\beta_2+\beta_p)} \tag{90}$$

Therefore, the real power P_p dissipated in the plasma is given by

$$\frac{P_p}{P_i} = \frac{4\beta_1\beta_p}{(1+\beta_1+\beta_2+\beta_p)^2 + \left[2Q_o \frac{\Delta\omega - \delta\omega}{\omega_o}\right]^2} \tag{91}$$

We can express β_p and $\delta\omega$ in terms of the electron density n and the collision frequency ν_c of the plasma, using Eqs. 57 and 58. If we assume that $\nu_c \ll \omega$, these equations may be written

$$\delta\omega = -\frac{c}{2}\frac{K_g\omega_o}{\omega_p} \tag{92}$$

and

$$\beta_p = \frac{Q_o c K_g}{\omega_p}\frac{\nu_c}{2\omega_o} \tag{93}$$

Experimentally, it was found that the electron density n is proportional to the amount of power that is dissipated in the discharge, or

$$n = K_1 P_p \tag{94}$$

Upon substituting Eqs. 92, 93, and 94 in Eq. 91, we obtain

$$\frac{P_p}{P_i} = \frac{P_p^{1/2} 2\beta_1 K_2 \nu_c/\omega_o}{\left[(1+\beta_1+\beta_2)K_2 P_p^{1/2} + \nu_c/2\omega_o\right]^2 + \left[P_p^{1/2} K_2 2Q_o(\Delta\omega/\omega_o) - 1\right]^2} \tag{95}$$

where

$$K_2 = \frac{\left[K_1 e^2/(m\epsilon_o)\right]^{1/2}}{2Q_o c K_g} \tag{96}$$

Equation 95 must be satisfied if the system is to operate stably. Solutions of this equation for P_p as a function of P_i for parametric values of Δf and $\frac{\nu_c}{\omega}$ are shown in Fig. 17. The parameters of Eq. 95 were obtained from the data of Table I and the curves of Fig. 22.

These curves explain many of the experimental phenomena that were noted in the course of this research. At low values of incident power, the power dissipated in the plasma is small – most of the incident microwave energy being reflected. This

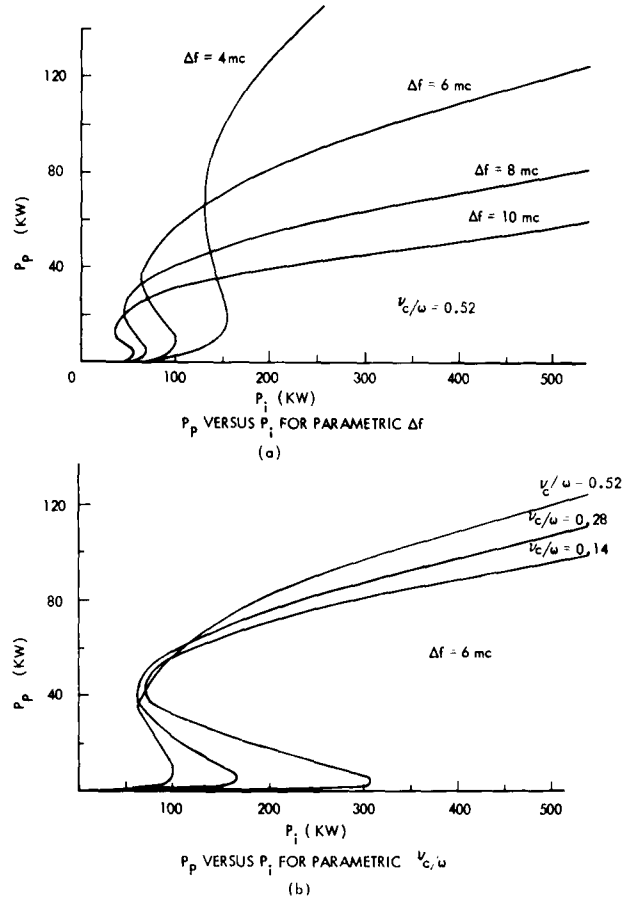

Fig. 17. P_p versus P_i for: (a) parametric Δf; (b) parametric ν_c/ω.

corresponds to operation in state 1. As the incident power is increased, the operating point shifts to a region at which three values of P_p satisfy Eq. 95 at the same value of P_i. However, if this region is approached from low incident powers, the system will operate in state 1. As the incident power is increased further, the operating point moves to the knee of the curves and then jumps to a much higher value of P_p, corresponding to operation in state 2. Further increases in P_i increase only slightly the amount of power dissipated in the discharge. These conclusions agree with experimental observations.

From Fig. 17(a), it can be seen that at constant incident power, when the system is operating in state 2, P_p is a strong function of Δf, particularly when Δf becomes small. As Δf decreases, it also becomes more difficult for the system to operate in state 2, as can be seen from the increasing values of P_i where the curve knee occurs.

The behavior of the system resulting from changes in electron collision frequency can be seen from Fig. 17(b). As the collision frequency is decreased by lowering the pressure, it becomes more difficult for the system to operate in state 2. This

effect was also noted experimentally.

In Section II, it was assumed that the series element β_s in the equivalent circuit of the cavity could be neglected. In section 2.5, it was shown that the conditions under which this assumption was most likely to be valid were that (i) $\delta\omega$ equals $\Delta\omega$ and (ii) the plasma is very dense and therefore a good conductor. An inspection of Fig. 17 shows that these conditions are most nearly fulfilled when the system is operated in state 2.

3.4 MICROWAVE CHARACTERISTICS

The microwave characteristics of the resonant cavity and coaxial plasma were studied experimentally.

Figure 18 shows plots of the S-band power absorbed by the cavity versus frequency for various gas pressures and values of incident power. When these curves were obtained, the incident power and the neutral-gas pressure were held constant and the excitation frequency was varied. Data were taken only when the discharge was operating in state 2.

The interesting feature of these curves is that as the excitation frequency approaches 2732 mc, a large portion of the incident power is coupled into the cavity. At relatively low powers, it was possible to couple over 90 per cent of the incident power into the cavity by adjusting the excitation frequency toward 2732 mc. At high incident powers, this was not possible because the sulfur hexafluoride that was used to pressurize

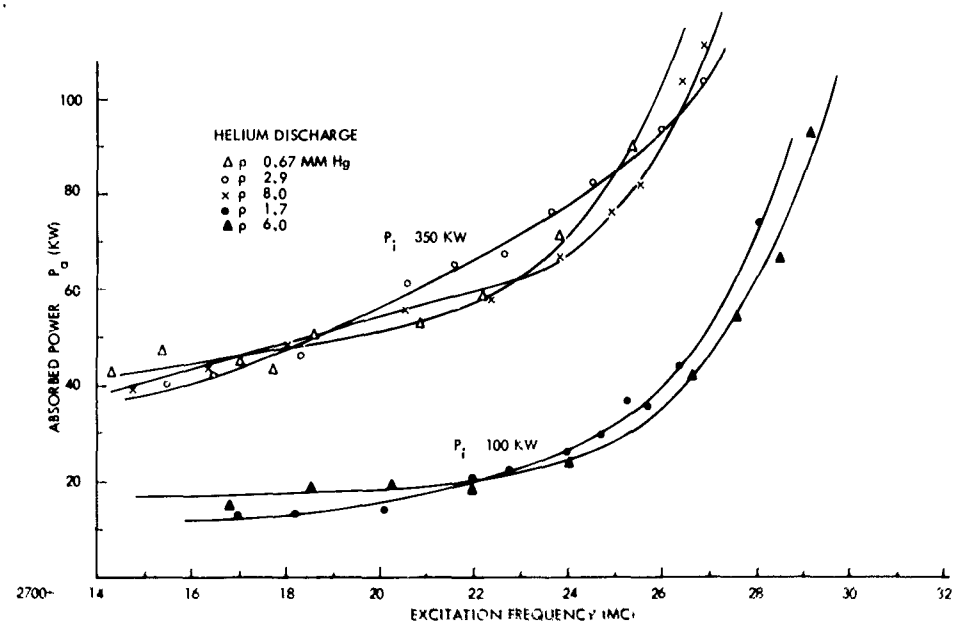

Fig. 18. Absorbed power as a function of excitation frequency for incident powers of 100 and 350 kw. The system is operating in state 2.

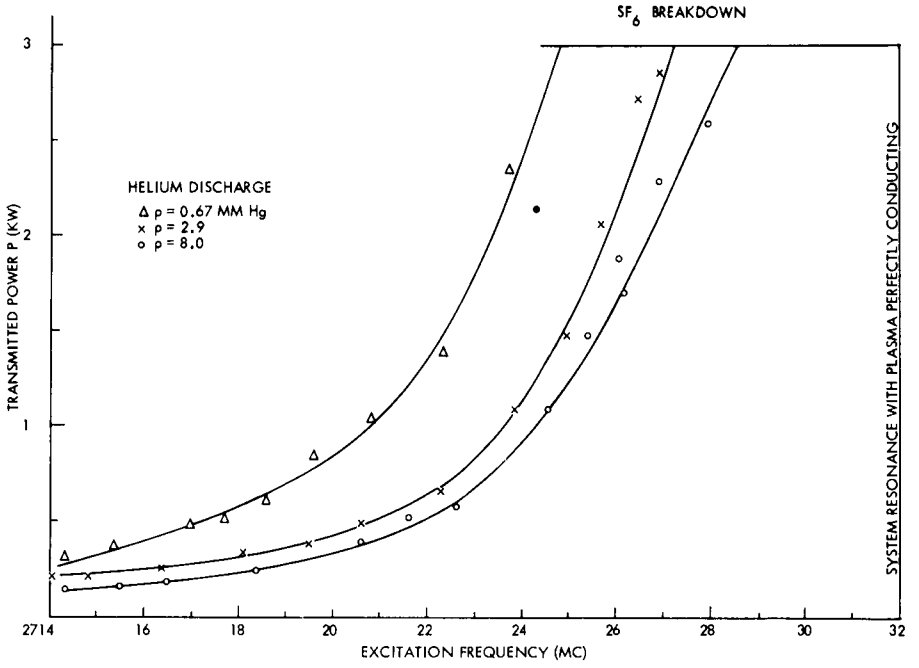

Fig. 19. Transmitted power as a function of excitation frequency for an incident power of 350 kw. The system is operating in state 2.

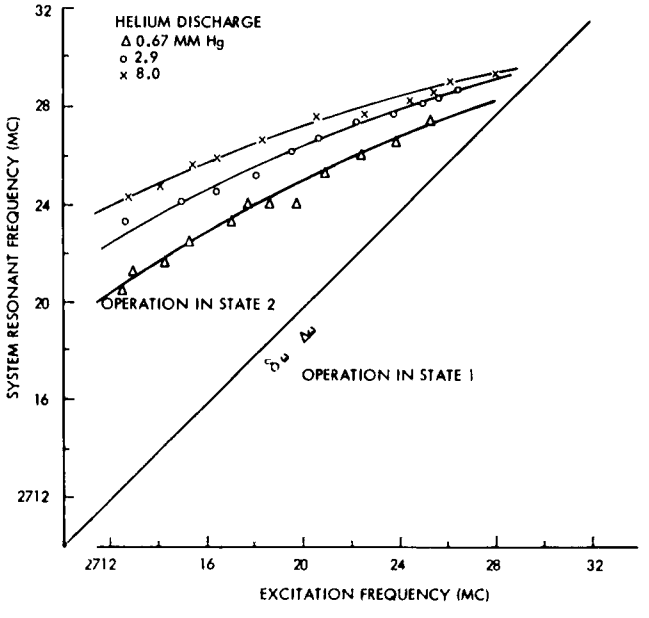

Fig. 20. System resonant frequency as a function of excitation frequency for an incident power of 350 kw.

the cavity would break down.

Figure 19 shows the way in which the S-band power transmitted through the cavity varies with frequency. As before, these curves were obtained when the gas pressure and incident power were held constant and the excitation frequency was varied.

The magnitude of the microwave field inside the cavity is proportional to the square root of the power transmitted through the cavity. Therefore, the variation of the microwave field with excitation can be obtained from Fig. 19.

Figure 20 shows how the system resonant frequency changes with excitation frequency at constant incident power. These curves were calculated from the data shown in Figs. 18 and 19 with the aid of Eq. 87. The line where $\delta\omega$ equals $\Delta\omega$ separates state 1 from state 2.

3.5 ELECTRON-DENSITY AND COLLISION-FREQUENCY MEASUREMENTS

The averaged electron density n_a and the collision frequency ν_c of the plasma column which formed the center conductor of the resonant cavity were calculated for several values of gas pressure, using measurements of S- and C-band quantities. The theory used for calculating these parameters is presented in Section II. The data presented here are the results of the better experiments which were performed.

Several experiments were performed at neutral-gas pressures of less than 0.6 mm Hg, but the results of these experiments were inconclusive. It is felt that experiments conducted at gas pressures below 1 mm Hg cannot be interpreted with the simple theory presented in this report. At low pressures, the mean-free path of an electron becomes comparable with the dimensions of the quartz tube and an electron may suffer more collisions with the walls than with the neutral gas particles. The theory of Section II assumes that the effects of electron-wall collision are negligible as compared with electron-neutral collisions; therefore, this theory is not valid at low gas pressures.

a. Electron-Density Measurements

Figure 21 shows graphs of the geometrically averaged electron density as a function of the peak power absorbed in the discharge at the pressures indicated. In each graph, the results of calculations based on both S- and C-band measurements are given for comparison. These curves were obtained by holding the pressure and incident power constant and varying the frequency of the microwave energy, as done in the phase of the experiment discussed in section 3.4.

The experimental error present in these curves is believed to be quite large (probably as large as 100 per cent). The largest errors are believed to occur in the measurement of the power absorbed by the plasma and in the electron density obtained from S-band measurements.

There are two sources of error which become important when the VSWR in the

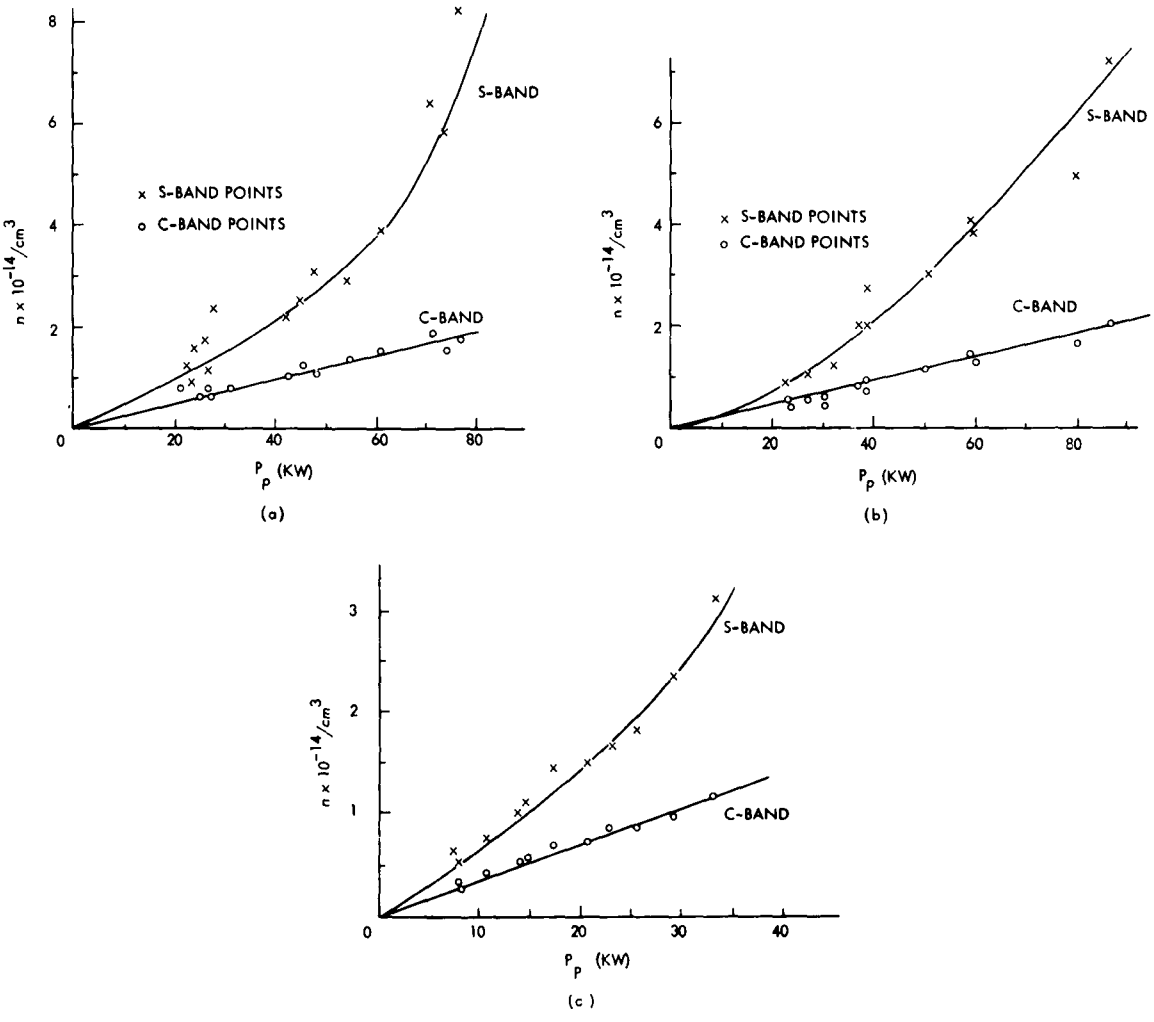

Fig. 21. Electron density vs plasma power with the helium discharge at pressures: (a) 8.0 mm Hg; (b) 2.9 mm Hg; (c) 1.7 mm Hg.

S-band waveguide is large. First, it is difficult to measure large standing-wave ratios for reasons pointed out in section 3.2; and second, the theory that is used to calculate n and P_p assumes that the effects of the off-resonant modes can be neglected. In section 2.5, it was shown that this assumption was most likely to be valid when the system is excited near resonance and the plasma electron density is large. This is equivalent to requiring a small standing-wave ratio in the S-band waveguide.

The C-band curves show an interesting relation. A reasonable curve fit to the C-band points is a straight line passing through the origin. A simple consideration of how energy escapes from the plasma tube predicts that, if recombination is not a significant factor, the electron density and the power absorbed by the discharge are linearly related (for instance, see Allis[26]). However, these considerations do not allow

the electron density to increase faster than the power absorbed by the plasma, as indicated by the S-band curves.

The fact that the electron density calculated from S-band measurements is larger than that calculated from C-band measurements is easily explained. The electron density measured is actually a geometrically averaged density at the plasma surface and is given by

$$n_a = \left[\frac{\int_{\text{plasma}} \left|\bar{H}_o\right|^2 da}{\int_{\text{plasma}} n^{-1/2} \left|\bar{H}_o\right|^2 da} \right]^2 \tag{97}$$

where n is the actual electron density. This equation is obtained from Eq. 54.

In general, the averaged electron density that is obtained from calculations based on C-band measurements will differ from n_a that is obtained from S-band measurements because of the different field patterns of the two cavity modes. The C-band mode weights the electrons on the plasma surface near the center of the quartz tube most heavily. The $\bar{H}$ field of the S-band mode is strongest at the plasma boundary near the cavity end walls. Since the power coupled to the plasma by the TE_{111} mode actually produces the discharge, the electron density is largest near the cavity end plates. Therefore, n_a measured with the S-band mode should be larger than n_a measured with the C-band mode.

b. Collision-Frequency Measurements

The collision frequency of the plasma column was also calculated as a function of the power dissipated in the discharge from measurements of S- and C-band parameters. The results of some of these calculations appear in Fig. 22. In this figure, the collision

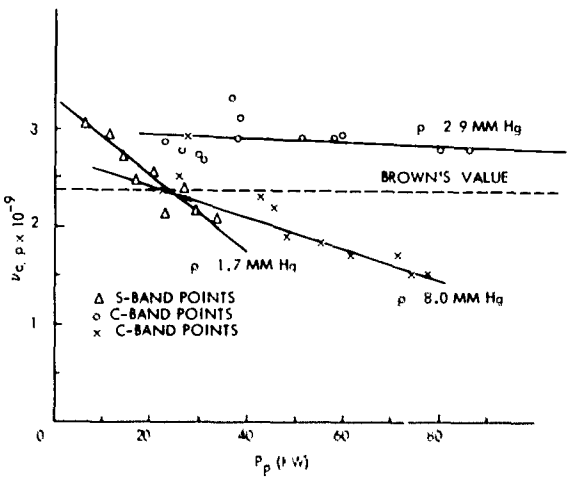

Fig. 22. ν_c/p as a function of P_p.

frequency has been normalized to the neutral-gas pressure, so that data obtained at different gas pressures could be compared. The most generally accepted value of collision frequency for helium[23] is

$$\nu_c = 2.37 \times 10^9 p \tag{98}$$

and is presented in Fig. 22 as a dashed line for comparison.

The negative slopes of the curves displayed in Fig. 22 are believed to be caused by heating of the gas contained in the quartz tube. The collision frequency is actually proportional to the neutral-gas density rather than pressure as indicated in Eq. 90. At constant pressure, the gas density varies inversely as the gas temperature; therefore, the collision frequency may be written

$$\nu_c/p = (\nu_{co}/p)(T_o/T) \tag{99}$$

where ν_{co} is the collision frequency at a pressure of p millimeters of mercury and a gas temperature of T_o degrees Kelvin.

One other phenomenon has been observed which supports the conclusion that the microwave power is heating the neutral gas in the tube and changing the neutral-gas density. The most sensitive parameter observed in these experiments was the time τ at which a transition from state 1 to state 2 occurs. When the excitation frequency and the incident power were adjusted so that a transition from state 1 to state 2 occurred at 4 or 5 μsec, the time at which the transition occurred would gradually increase until it was greater than 10 μsec, and no transition occurred after the power had been applied 10 or 15 seconds. It was then necessary to increase the incident microwave power or decrease the excitation frequency to allow the transition to be observed again. Figure 17(b) shows that as ν_c decreases, more incident power is required for the system to operate in the second state. Therefore, this behavior can be explained by a decrease in the electron collision frequency which results from a heating of the neutral gas.

3.6 LIGHT EXPERIMENTS

Visual observations of the light generated by the discharge showed that the discharge was brightest in a thin, 1-mm shell at the surface of the plasma. Figure 23 shows this discharge; taken with a pinhole camera from the top of the cavity, this photograph gives a view downward toward the C-band waveguide. The elliptical dark spot in the center is a distortion of the C-band coupling hole which was caused by the quartz tube.

The interesting feature of the spatial distribution of the light generated by the plasma is that the light is brightest where the transverse magnetic field of the TE_{111} coaxial mode is maximum. This is not surprising because the microwave power per unit area which goes into the plasma is given by

$$P = \frac{1}{2} \text{Re} \left[Z_p |\overline{H}|^2 \right] \tag{100}$$

Thus, the spatial dependence of the generated light supports the conclusion that the cavity was resonating in the TE_{111} coaxial mode.

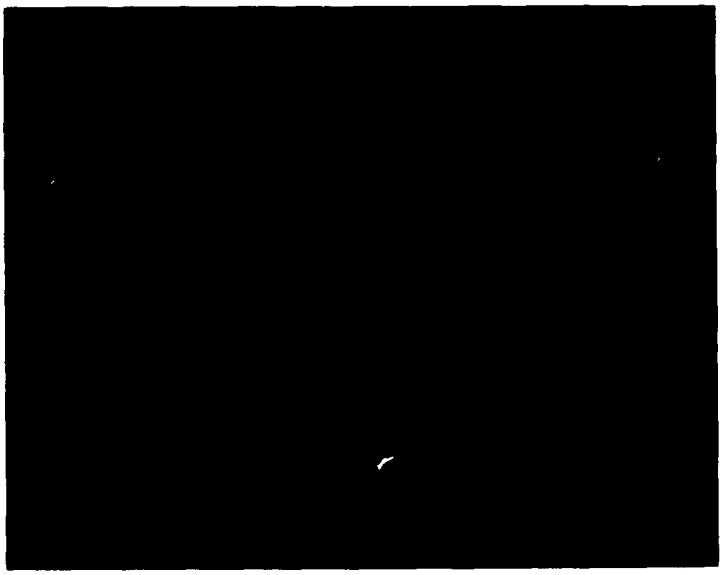

Fig. 23. Light generated by the discharge as viewed from the top.

The light generated by the discharge also shows that the electron density is not uniform over the surface of the plasma. One would expect the electron density to be largest where the generated light is greatest. This conclusion was also reached from measurements of the averaged electron density of the discharge based on measurements of S- and C-band parameters in section 3.5a.

The light generated by the discharge was studied as a function of time with the aid of a photomultiplier tube and an oscilloscope. Figure 24 contains oscillograms of the light intensity versus time which were generated by helium discharges at gas pressures of 1, 2, 4, and 8 mm Hg. The time scales of these oscillograms are 5 μsec per large division. At each pressure, the incident power and excitation frequency were adjusted to a point at which the sulfur hexafluoride used to pressurize the cavity was just on the verge of breaking down. Thus the power absorbed by the discharge was maximized. The gain of the oscilloscope and phototube circuit was the same in each picture so that relative comparisons of light intensity can be made.

There are several interesting features of the wave shapes of the light intensity which have been observed: (a) the largest light intensity occurred briefly just at the time a transition from state-1 operation to state-2 operation was observed; (b) the light intensity during the microwave pulse is not strongly dependent on the amount of

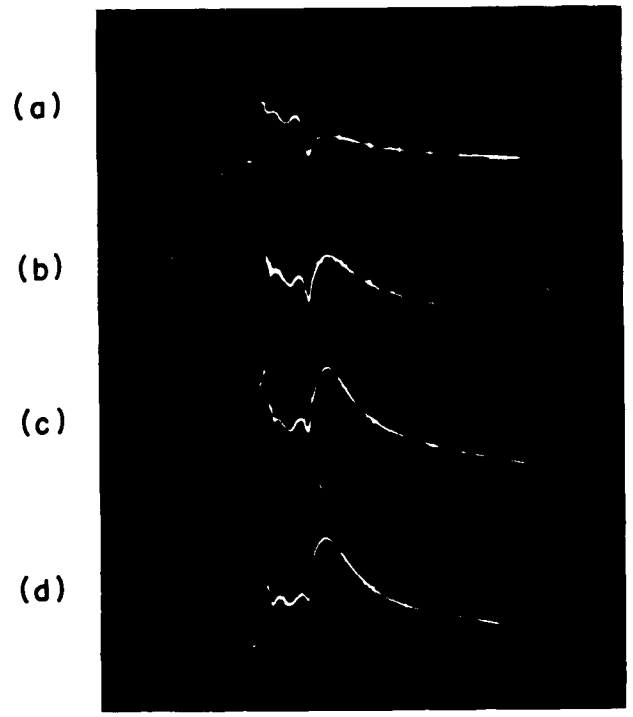

Fig. 24. Oscillograms of light generated by the helium discharge at pressures: (a) 1 mm Hg; (b) 2 mm Hg; (c) 4 mm Hg; (d) 8 mm Hg. The time scale is 5 μsec/cm.

power dissipated in the plasma; (c) the light generated by the discharge decreases sharply when the microwave energy ceases (τ = 10 μsec) and then increases rapidly with an initial slope that is proportional to pressure; and (d) the afterglow light is quite sensitive to the neutral-gas pressure and to the power dissipated in the plasma. At low power levels or pressure levels, the waveforms of generated light intensity versus time were similar to those of Fig. 8(d). The physical processes occurring in the discharge, which cause the above phenomena, are not understood.

A monochrometer was used to examine the spectral lines generated by a helium discharge. The resolution of the monochrometer was approximately 1 Å. The spectrum was examined in the region of 2000-8000 Å. In this region, lines originating from the excitation of oxygen and silicon, as well as helium, were observed.

Figure 25 shows oscillograms of the magnitude of the microwave field inside the cavity, the total light generated by the discharge, the 4471 helium line, and the 5056 silicon line. These oscillograms were taken of a helium discharge at a pressure of 1.9 mm Hg. A transition from state-2 operation occurred at τ = 6 μsec. The discharge was excited with 170 kw of peak microwave power at a frequency of 2728 mc. The frequency response of the phototube circuit used for obtaining the oscillograms, Fig. 25(c) and (d), was insufficient to obtain accurate plots of light versus time. Stray pickup in

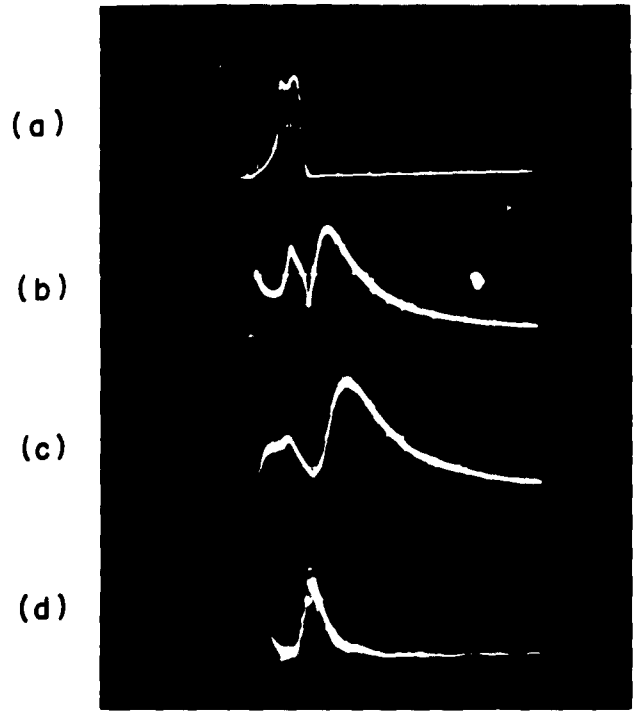

Fig. 25. Oscillograms of a helium discharge in a resonant cavity showing wave shapes of: (a) the microwave-field intensity inside the cavity; (b) total light generated; (c) the 4471 helium line; and (d) the 5056 silicon line. A transition from state 1 to state 2 occurs at $\tau = 6$ μsec. The time scale is μsec/cm.

the phototube circuit accounts for the initial deflection of the oscilloscope trace shown in Fig. 25(d).

The shapes of other helium and silicon lines observed were similar to those presented in Fig. 25. The waveforms of the oxygen lines were similar to those of the helium lines.

These observations indicate that silicon and oxygen are being strongly excited when the discharge is operating in state 2 and may be poisoning the discharge.

IV. CONCLUSIONS

4.1 RESULTS

In this report we have investigated a method of producing a dense plasma with high-power pulsed microwave energy. The principal results demonstrated by the experiments are threefold and may be summarized as follows:

a. A large amount of microwave energy can be dissipated in a dense plasma, with a resonant cavity used to couple the energy into the plasma.

b. A dense plasma in a resonant cavity should be considered as a lossy conductor, rather than as a lossy dielectric, when calculating the effects of the plasma on the microwave properties of the cavity.

c. The initial transient in the plasma electron density, when the microwave power is first applied, occurs very rapidly and measurements on a plasma produced in 10 μsec by a microwave pulse can be performed with little difficulty.

4.2 POSSIBLE SOLUTIONS TO PROBLEMS ENCOUNTERED

The amount of microwave power which could be coupled into the plasma was first limited by breakdown of the sulfur hexafluoride used to pressurize the cavity. There are several methods that can be used to prevent SF_6 breakdown. One method would be to increase the pressure of the SF_6; a second would be to choose a cavity mode that couples more strongly to the plasma.

A second problem encountered in this work was the difficulty of measuring the neutral-gas density in the volume occupied by the plasma. The pulsed discharge causes pressure transients in the plasma, and, consequently, measurements of the pressure in other parts of the system do not give the neutral-gas density in the plasma.

There was experimental evidence that the discharge was being contaminated by impurities given off by the quartz tube. This is doubly important because the strongest microwave interaction occurs at the plasma surface where the impurity concentration is greatest. The only way to eliminate these impurities is to eliminate the quartz tube, and then it would be necessary to confine the plasma with electric or magnetic fields.

A change of cavity modes would do much to simplify the interpretation of the experiments and provide better results. In the absence of an axial magnetic field, the best mode to use to drive the discharge is the TM_{010} coaxial mode. The TE_{020} coaxial mode could then be used to probe the plasma. This combination of modes would provide the greatest amount of symmetry in the fields that exist on the plasma surface. The only electron-density gradients induced by these modes would be normal to the quartz tube.

The addition of the proper dc magnetic field along the cavity axis would increase the plasma electron density that could be obtained, for two reasons. First, the magnetic field would reduce the radial diffusion to the quartz wall; and second, the field could be

adjusted so that the plasma is driven at cyclotron resonance. The reduction of the radial diffusion to the wall would result in a higher electron density at a given power by reducing the rate at which electrons (and, therefore, energy) are lost from the discharge. Adjusting the magnetic field so that the electron cyclotron frequency equals the applied frequency would, in effect, couple the plasma center conductor more strongly to the cavity mode. Thus, more power could be coupled into the cavity without breaking down the SF_6. Also, the discharge could be operated at lower gas pressures, since collisions are not required to couple microwave energy into a plasma at cyclotron resonance.[27]

The electric field in the plasma must be perpendicular to the dc magnetic field if the plasma is to be driven at cyclotron resonance. Consequently, the choice of cavity modes is important. If the magnetic field is directed along the cavity axis, the mode which provides the greatest symmetry and also a strong circular electric field in the plasma is the TE_{011} coaxial mode.

4.3 SUGGESTIONS FOR FUTURE EXPERIMENTAL WORK

a. More measurements of electron density and collision frequency as a function of power absorbed in the discharge and neutral-gas pressure should be performed with the existing apparatus, to investigate the loss processes which control the discharge.

b. An experiment should be performed to measure the electron density in the plasma column, which would provide a check on the method devised in this work. A simple method would be to measure the transmission of a very high frequency microwave signal through the resonant cavity with and without the plasma. The plasma becomes opaque to the microwave energy when the plasma frequency becomes greater than the applied frequency. Thus, the plasma frequency could be measured by observing the lowest frequency of the microwave energy at which the transmission through the resonant cavity is affected by the discharge. A microwave frequency of approximately 90 kMc is required to measure an electron density of 10^{14} per cm^3 using this method.

c. It should be possible to make Langmuir-probe measurements[28] on the plasma by placing the probe along the cavity axis. Since the microwaves do not penetrate far into the plasma, little microwave energy should be coupled out of the cavity by the probes. A probe measurement would check the measurement of electron density with microwave energy and would provide a measure of the plasma electron temperature.

4.4 SUGGESTIONS FOR FUTURE THEORETICAL WORK

a. One of the most important theoretical calculations which should be performed is a computation of the effects of a finite electron-density gradient, normal to the plasma surface, on the perturbation theory developed in Section II. It is felt that the electron-density gradients at the plasma surface may be contributing a large error to the experiments described in section 3.5.

b. The perturbation theory of Section II should be generalized to include the effects of a dc magnetic field acting on the plasma.

c. The loss processes that control the discharge should be studied and an attempt made to calculate theoretically the plasma electron density as a function of absorbed power.

d. The time dependence of the transition from operation in state 1 to operation in state 2 should be studied quantitatively.

APPENDIX

DETERMINATION OF β_1, β_2, AND Q_o FOR THE TE_{111} COAXIAL MODE

The theory of Section II assumed that the microwave parameters of the resonant cavity were known when the volume normally occupied by the plasma was replaced by a perfect conductor. The parameters of the cavity were obtained by filling the quartz tube with mercury and measuring the cavity parameters by standard microwave methods. Since mercury is not a perfect conductor, it was necessary to eliminate the effects of the loss in the mercury. The details of this calculation are presented here.

The perturbation analysis of Section II can be applied directly to the treatment of loss in the mercury center conductor. From Eq. 43 we have

$$\frac{\Delta f}{f_o} = \frac{-K_g \, \mathrm{Im}\,(Z_m)}{2\mu_o \omega_o} \tag{101}$$

and from Eq. 47

$$\frac{1}{Q_m} = \frac{K_g \, \mathrm{Re}\,(Z_m)}{\mu_o \omega_o} \tag{102}$$

where K_g is defined by Eq. 57 and Z_m is the wall impedance of mercury and is given by

$$Z_m = \left[\frac{j\omega\mu_o}{\sigma_m}\right]^{1/2} \tag{103}$$

where σ_m is the conductivity of mercury which is 1.04×10^4 mhos/cm.

For the TE_{111} coaxial mode of the cavity used in this research, we find

$$\begin{aligned} \Delta f &= -60\ 6 \text{ kc} \\ Q_m &= 22,700 \end{aligned} \tag{104}$$

and for the TE_{011} coaxial mode,

$$\begin{aligned} \Delta f &= -93.0 \text{ kc} \\ Q_m &= 23,100 \end{aligned} \tag{105}$$

The loaded Q_l, the VSWR ρ_o at resonance, and the ratio R of the transmitted power to the absorbed power were measured with the mercury present. If the cavity is overcoupled, we obtain, from the equivalent circuit of Fig. 3(b),

$$\rho_o = \frac{\beta_1}{1 + \beta_2 + \beta_m} \tag{106}$$

$$R = \frac{\beta_2}{1 + \beta_2 + \beta_m} \tag{107}$$

and

$$Q_o = (1+\beta_1+\beta_2+\beta_m)\, Q_\ell \tag{108}$$

where Q_o is the unloaded cavity Q, β_1 and β_2 are, respectively, the input and output coupling coefficient, and β_m is the mercury coupling coefficient which is defined by

$$\beta_m = \frac{Q_o}{Q_m} \tag{109}$$

If we solve Eqs. 106-109 for β_1, β_2, and Q_o, we obtain

$$Q_o = \frac{Q_\ell(1+\rho_o)}{1 - R - (Q_\ell/Q_m)(1+\rho_o)} \tag{110}$$

$$\beta_1 = \frac{\rho_o}{1 - R - (Q_\ell/Q_m)(1+\rho_o)} \tag{111}$$

and

$$\beta_2 = \frac{R}{1 - R - (Q_\ell/Q_m)(1+\rho_o)} \tag{112}$$

Equations 110-112 were obtained under the assumption that the cavity is overcoupled to the microwave source. If the cavity is undercoupled, these equations may be used if the reciprocal of the measured VSWR is substituted for ρ_o wherever it appears.

The microwave parameters presented in Table I were calculated from measurements of Q_ℓ, ρ_o, and R, by using Eqs. 110-112.

Acknowledgments

The author is sincerely grateful for the supervision and advice of Professor L. D. Smullin, and for the helpful suggestions of his fellow-students, Ward D. Getty and Paul Chorney, during the course of this project. Thanks are due Professor D. R. Whitehouse for several enlightening discussions.

The author also wishes to thank Francis W. Barrows and Harry D. Gay for their aid in constructing the apparatus, and Lawrence W. Ryan and other members of the Machine Shop of the Research Laboratory of Electronics for fabricating the glass portions of the apparatus.

References

1. D. J. Rose, D. E. Kerr, M. A. Biondi, E. Everhart, and S. C. Brown, Methods of Measuring the Properties of Ionized Gases at High Frequencies, Technical Report 140, Research Laboratory of Electronics, M.I.T., October 17, 1949.
2. J. C. Slater, Microwave Electronics (D. Van Nostrand Company, Inc., Princeton, N. J., 1950), pp. 66-67.
3. K. B. Persson, Limitations of the microwave cavity method of measuring electron densities in a plasma, Phys. Rev. 106, 191-195 (1957).
4. S. J. Buchsbaum and S. C. Brown, Microwave measurements of high electron densities, Phys. Rev. 106, 196-199 (1957).
5. S. J. Buchsbaum, L. Mower, and S. C. Brown, Interaction between cold plasmas and guided electomagnetic waves, Phys. Fluids 3, 806-819 (1960).
6. H. Hsieh, J. M. Goldey, and S. C. Brown, A resonant cavity study of semiconductors, J. Appl. Phys. 25, 302-307 (1954).
7. S. J. Buchsbaum, Interaction of Electromagnetic Radiation with a High Density Plasma, Ph.D. Thesis, Department of Physics, M.I.T., January 1957.
8. S. C. Brown and D. J. Rose, Methods of measuring the properties of ionized gases at high frequencies. I. Measurements of Q, J. Appl. Phys. 23, 711-718 (1952).
9. D. J. Rose and S. C. Brown, Methods of measuring the properties of ionized gases at high frequencies. II. Measurements of electric field, J. Appl. Phys. 23, 719-722 (1952).
10. D. J. Rose and S. C. Brown, Methods of measuring the properties of ionized gases at high frequencies. III. Measurements of discharge admittance and electron density, J. Appl. Phys. 23, 1028-1032 (1952).
11. L. Gould and S. C. Brown, Methods of measuring the properties of ionized gases at high frequencies. IV. A null method of measuring the discharge admittance, J. Appl. Phys. 24, 1053-1056 (1953).
12. M. A. Biondi and S. C. Brown, Measurements of ambipolar diffusion in helium, Phys. Rev. 75, 1700-1705 (1949).
13. A. V. Phelps, O. T. Fundingsland, and S. C. Brown, Microwave determination of the probability of collision of slow electrons in gases, Phys. Rev. 84, 559-562 (1951).
14. E. Everhart and S. C. Brown, The admittance of high frequency gas discharges, Phys. Rev. 76, 839-842 (1949).
15. W. P. Allis, S. C. Brown, and E. Everhart, Electron density distribution in a high frequency discharge in the presence of plasma resonance, Phys. Rev. 84, 519-522 (1951).
16. D. J. Rose and S. C. Brown, High frequency gas discharge plasma in hydrogen, Phys. Rev. 98, 310-316 (1955).
17. S. J. Buchsbaum, Highly ionized plasmas, Quarterly Progress Report, Research Laboratory of Electronics, M.I.T., October 15, 1957, pp. 3-4.
18. M. P. Madan, E. I. Gordon, S. J. Buchsbaum, and S. C. Brown, Determination of the coefficients of diffusion and frequency of ionization in microwave discharges, Phys. Rev. 106, 839-843 (1957).
19. R. B. Brode, Quantitative study of the collisions of electrons with atoms, Rev. Mod. Phys. 5, 257-279 (1933).
20. S. C. Brown, High-Frequency Gas-Discharge Breakdown, Technical Report 301, Research Laboratory of Electronics, M.I.T., July 25, 1955.
21. J. C. Slater, op. cit., pp. 63-71.

22. R. Beringer, Resonant cavities as microwave circuit elements, Principles of Microwave Circuits, C. E. Montgomery, R. H. Dicke, and E. M. Purcell (eds.) (McGraw-Hill Book Company, Inc., New York, 1948), pp. 207-239.

23. S. C. Brown, Basic Data of Plasma Physics (John Wiley and Sons, Inc., New York, 1959), p. 143.

24. C. E. Muehe, Jr., A Simple Clean Pressure Gauge for the Millimeter Range, Lincoln Laboratory Group Report 46-47, M.I.T., 18 November 1959, pp. 46-47.

25. W. L. Teeter and K. R. Bushore, A variable-ratio microwave power divider and multiplier, IRE Trans. MTT-5, 227-229 (1957).

26. W. P. Allis, Power Balance, Report No. LA-2055, Los Alamos Scientific Laboratory, University of California, Los Alamos, N.M. (1956).

27. W. P. Allis, Notes on Plasma Dynamics, Summer Session Lecture Notes, M.I.T., 1959, pp. A-5-A-10 (unpublished).

28. H. M. M. Smith and I. Langmuir, The theory of collectors in gaseous discharges, Phys. Rev. 28, 727-763 (1925).